Full-Duplex Two-Way and One-Way Relaying: Average Rate, Outage Probability, and Tradeoffs

Zhengquan Zhang, Zheng Ma, *Member, IEEE*, Zhiguo Ding, *Senior Member, IEEE*, Ming Xiao, *Senior Member, IEEE*, and George K. Karagiannidis, *Fellow, IEEE*

***Abstract*—In this paper, we systematically study the average rate and outage probability tradeoffs of full-duplex two-way and one-way relaying under residual self-interference. Among various relaying protocols, two common of them are considered: amplify-and-forward (AF) and decode-and-forward (DF). Furthermore, we consider the application of physical-layer network coding (PNC) and analog network coding (ANC) to full-duplex two-way relaying. Novel closed-form expressions for the average rate and outage probability, are presented. The results show that full-duplex two-way relaying can achieve higher rate than one-way relaying in the medium to high signal-to-noise ratio (SNR) region, at the cost of a certain loss in the outage performance. Moreover, DF protocol can achieve better outage performance than the AF one, but it suffers from a certain loss in the rate in the high SNR region. It is also shown that PNC can further improve the rate and outage performance. In addition, the results clearly reveal the effects of time multiplexing, forward protocol, and network coding on relaying systems, which would shed light on designing practical full-duplex relaying schemes.**

***Index Terms*—Full duplex relaying, time multiplexing, network coding, average rate, outage probability.**

I. Introduction

SPECTRUM efficiency is a crucial aspect for wireless communication systems, because of the limited spectrum resources used to satisfy the increasing data rate demands. To distinguish the uplink and downlink, duplex techniques are adopted as resource sharing solutions. In most of the wireless systems, available resources (time, frequency, etc.) are used to support bidirectional transmission. However, recently, full-duplex radio was proposed as a promising technique for the next generation wireless communication systems, because it can double the spectrum efficiency by achieving transmission and reception on the same carrier frequency, simultaneously [1]–[6]. In addition, relaying technique, which enables the wireless network to work in a cooperative manner, is also an efficient way to improve the spectrum efficiency and extend the coverage. Half-duplex relaying like four-slot and two-slot schemes attracts wide research [7]–[13], and it has already been adopted in the fourth-generation (4G) wireless networks [14], [15]. Full-duplex relaying, which integrates the merits of full-duplex radio and relaying, can further improve the spectrum efficiency. Currently, there are two potential full-duplex relaying schemes, named full-duplex one-way relaying (FD-OWR) [16] and full-duplex two-way relaying (FD-TWR) [17], [18]. In such relaying systems, network coding technique can be taken into consideration to improve the system performance. Scanning the open literature, two common network coding schemes, named physical-layer network coding (PNC) [19] and analog network coding (ANC) [20], were proposed to improve the throughput in multi-hop wireless networks.

Manuscript received May 26, 2015; revised October 22, 2015 and January 13, 2016; accepted February 2, 2016. Date of publication February 18, 2016; date of current version June 7, 2016. This work was supported in part by the National Basic Research Program of China under Grant 2012CB316100, in part by the National Natural Science Foundation of China under Grant 61571373, in part by the National High Technology Research and Development Program of China under Grant 2014AA01A707, in by the Key Grant Project of Chinese Ministry of Education under Grant 311031100, in part by the Young Innovative Research Team of Sichuan Province under Grant 2011JTD0007, and in part by the National Natural Science Foundation of China under Grant 61371105. The work of Z. Ding was supported by the U.K. EPSRC under Grant EP/L025272/1. The associate editor coordinating the review of this paper and approving it for publication was D. C. Popescu.

Z. Zhang and Z. Ma are with the Key Laboratory of Information Coding and Transmission, Southwest Jiaotong University, Chengdu 610031, China (e-mail: zhang.zhengquan@hotmail.com; zma@home.swjtu.edu.cn).

Z. Ding is with the School of Computing and Communications, Lancaster University, Lancaster LA1 4YW, U.K. (e-mail: z.ding@lancaster.ac.uk).

M. Xiao is with the Department of Communications Theory, School of Electrical Engineering, Royal Institute of Technology (KTH), Stockholm 10044, Sweden (e-mail: mingx@kth.se).

G. K. Karagiannidis is with the Key Laboratory of Information Coding and Transmission, Southwest Jiaotong University, Chengdu 610031, China, and also with the Department of Electrical and Computer Engineering, Aristotle University of Thessaloniki, Thessaloniki 54124, Greece (e-mail: geokarag@auth.gr).

Color versions of one or more of the figures in this paper are available online at http://ieeexplore.ieee.org.

Digital Object Identifier 10.1109/TWC.2016.2531050

A. Related Work

Compared with half-duplex relaying, FD-OWR can offer higher system capacity, by achieving unidirectional data transmission and reception on the same carrier frequency simultaneously, even though it suffers from residual self-interference at the relay. In [16], Riihonen et al. studied the capacity tradeoff between the amplify-and-forward (AF) based FD-OWR with residual self-interference and the half-duplex relaying, under the assumption of absence of fading in the source-relay and residual self-interference channels. This rate-interference tradeoff between the decode-and-forward (DF) based FD-OWR and half-duplex relaying were also studied under the same assumption [21]. In [22], Hu et al. also studied this capacity tradeoff between the AF based FD-OWR and half-duplex relaying, by assuming that the source-relay channel was subjected to fading. In the same work, the outage probability was also derived, under the assumption that there was no direct link between the source and destination nodes. In [23], Riihonen et al. proposed two gain control schemes for the AF based FD-OWR protocol, which maximizes the signal-to-interference-plus-noise ratio

(SINR) and decreases the transmit power. Moreover, outage probability expressions were also derived, by considering the direct link as interference. In [24], Kwon et al. derived the outage probability of DF based FD-OWR under the same consideration, and studied the conditions to guarantee the superiority of full-duplex against half-duplex mode, under a certain target in the outage probability. Furthermore, in [25], Day et al. investigated the achievable rate for the DF based full-duplex multiple-input multiple-output (MIMO) one-way relaying. In the same work, residual self-interference, direct link, limited transmitter/receiver dynamic range and imperfect channel state information (CSI), were also taken into consideration. In another work, Riihonen et al. proposed a combination of opportunistic full-duplex/half-duplex mode selection and transmitted power adaptation for maximizing the spectrum efficiency [26]. In [27], Krikidis et al. introduced a block-by-block transmission scheme, which ensured diversity gain at least equal to one, while the diversity-multiplexing tradeoff of AF without loop interference cancellation (LIC), AF with imperfect LIC, and DF with imperfect LIC, were also studied. In [28], Alves et al. compared the outage probability and system throughput of two-way half-duplex to one-way full-duplex relaying, and pointed out that FD-OWR could outperform bidirectional half-duplex relaying, even in the presence of self-interference. In [29], Alves et al. investigated the throughput and outage probability of a full-duplex block Markov relaying scheme with self-interference at the relay under independent non-identically distributed Nakagami-m fading. In [30], Rodriguez et al. investigated the pair-wise error probability, bit error rate (BER), and diversity performance of the AF based full-duplex linear relaying and dual-hop systems, under the effect of residual self-interference. In [31], Hong and Caire considered virtual full-duplex relaying by means of two half-duplex relays, which was a good alternative before standardizing full-duplex technology. In the same work, self-interference is replaced by inter-relay interference in this virtual version. In [32], Osorio et al. compared the outage probability of a variable-gain AF based FD-OWR with direct link to half-duplex counterpart, and proposed a highly exact approximation to the outage probability. Finally, in [33], Liu et al. summarized the latest research progress, issues and challenges for FD-OWR.

FD-TWR can further improve system capacity by achieving bidirectional data transmission and reception on the same carrier frequency simultaneously. In [17], Rankov and Wittneben derived the achievable rate region for FD-TWR without residual self-interference, while in [34], Cheng et al. also derived this achievable rate region, but they assumed the existence of residual self-interference. In [18], Ju et al. studied the resource efficiency of two-way and full-duplex relaying systems, while in [35], Vaze and Heath studied the diversity-multiplexing tradeoff of FD-TWR, and proposed a compress and forward strategy to achieve the optimal diversity-multiplexing tradeoff. In [36], Choi and Lee studied the outage probability of the AF based FD-TWR with residual self-interference, in case of the perfect and imperfect CSI, and derived approximate closed-form expressions. In [37], Cui et al. proposed an optimal max-min relay selection scheme of the AF based relaying, and studied its BER, ergodic capacity, and outage probability. In the same work, an optimal power allocation and duplex mode selection to minimize the outage probability, was also presented. In [38], Cheng and Devroye studied the degree of freedom (DoF) of the K-pair-user with a MIMO relay. In [39], Tedik and Kurt proposed a full duplex PNC, in which the relay used detect-and-forward technique and the maximum likelihood (ML) based joint detection to eliminate the multiple access interference. In [40], Zhang et al. studied the capacity of two-way massive MIMO full-duplex relay systems, and pointed out that the very large antenna array could significantly reduce the effect of loop interference due to the antenna array gain. Finally, in [41], Chen et al. studied the spectral-energy efficiency tradeoff in a AF based FD-TWR network and developed a lower complexity iterative algorithm to solve the energy efficiency optimization problem, under the spectral efficiency requirement and the maximum transmission power constraints. However, there is still a lack in the literature regarding a detailed study of the performance tradeoff of various factors and relaying schemes, which affect the design of practical full-duplex relaying schemes.

B. Motivation and Contribution

In this paper, we study the average rate and outage probability tradeoffs of three-node model based FD-OWR and FD-TWR. The second one utilizes less time resources to exchange the same data, by multiplexing transmitting and receiving time, but it suffers from more severe residual self-interference, compared with FD-OWR. However, the effects of time multiplexing, residual self-interference, forwarding protocols, and network coding schemes on FD-TWR are unknown yet. In this work, we derive closed-form expressions for the average rate and outage probability, which are two important metrics in order to evaluate this effect. Since there are several relaying protocols with different processing mechanism, each of them has a different impact on the system behavior. Among these protocols, we consider AF and DF protocols, which have already been adopted in 4G wireless networks. Furthermore, two common network coding schemes, named PNC and ANC, are also considered, in the performance analysis of the DF based FD-TWR.

The contribution of this paper can be summarized as follows:

- We study two types of full-duplex relaying, full-duplex one-way and two-way relaying, and present novel closed-form expressions for the average rate and outage probability of the AF based FD-TWR and the DF based FD-TWR with PNC and ANC;
- A detailed performance analysis and a comparison between FD-TWR and FD-OWR are also proposed, and the effects of time multiplexing, forward protocols, and network coding schemes on the relaying systems, are also investigated.

C. Paper Outline

The remainder of this paper is organized as follows. Section II, describes the system model and includes the main notations used in this paper. A detailed derivation of the average rate and outage probability of FD-TWRs based, respectively, on

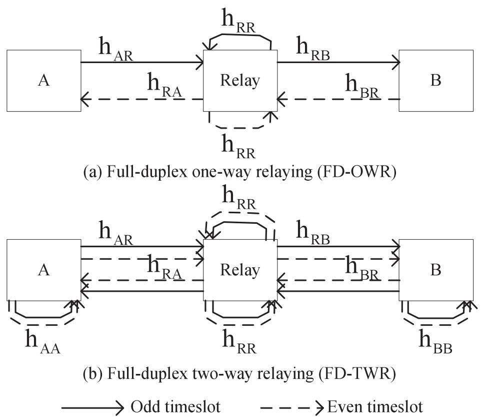

Fig. 1. System model of full-duplex two-way and one-way relaying.

AF and DF protocols, are presented in Section III. Analytical results, Monte Carlo simulations and discussions are presented in Section IV, followed by the conclusions in Section V.

II. System Model

A three-node FD-TWR model, which consists of two nodes A and B, and a relay, is considered in Fig. 1, with (a) FD-OWR and (b) FD-TWR. Due to imperfect interference cancellation, the residual self-interference in full-duplex nodes is taken into consideration. In addition, for the coverage extension scenarios, no direct link between source and destination nodes is assumed, due to transmit power limitation or the severe shadowing effect [14], [16], [37], [41]. In each time slot, FD-OWR can achieve unidirectional data transmission and reception between nodes A and B via the relay on the same carrier frequency, while FD-TWR can achieve bidirectional data transmission and reception. This means that FD-TWR can further multiplex the transmitting and receiving time, compared with FD-OWR. Moreover, only the relay in FD-OWR works in full-duplex, whereas all the nodes in FD-TWR operate in this mode. Therefore, FD-TWR would suffer from more severe self-interference, also called loop interference (LI), caused by the co-channel transmission and imperfect interference cancellation, compared with FD-OWR. Furthermore, FD-TWR is similar to half-duplex two-way relaying [7] and still consists of the multiple access (MAC) and broadcast (BC) stages. But, these stages in FD-TWR can be performed in parallel, in the same time slot and thus, all the nodes work in full-duplex mode and suffer from residual self-interference. In cellular networks, the node A, relay and node B, are denoted as the user equipment (UE), relay node (RN) and base station (BS), respectively.

Although the detrimental effect of self-interference can be mitigated by using multiple-stage interference cancellation [6], there is still residual self-interference, due to imperfections of radio frequency chains. According to previous works [2], [3], [16], [30], the variance of residual self-interference is approximately proportional to the λ-th power of the average transmitted power, where, $\lambda \in [0, 1]$, depends on the effect of the used self-interference cancellation techniques. In practice, the accurate relation between the transmitted power and the residual self-interference is still unknown [30]. Therefore, it is common to set it to an empirical value, which is obtained from field measurements.

The involved channels are node A$\rightarrow$relay (AR), relay $\rightarrow$node A (RA), node B $\rightarrow$relay (BR), relay $\rightarrow$node B (RB), and residual self-interference in node A, relay and node B. The corresponding channel coefficients are denoted as h_{AR}, h_{RA}, h_{BR}, h_{RB}, h_{AA}, h_{RR}, and h_{BB}, where h_{AR} and h_{BR} are independent and the incoming and outgoing channels are reciprocal, i.e., $h_{AR} = h_{RA}$ and $h_{BR} = h_{RB}$ [34], [37], [40], [41]. Similarly to [16], [22], the residual self-interference channels are assumed to be free of fading, while the AR, RA, BR, and RB channels are subjected to block Rayleigh fading. Thus, the instantaneous signal-to-noise ratio (SNR), γ, is an exponential random variable (RV), with probability distribution function (PDF), $f_{\bar{\gamma}}(\gamma) = (1/\bar{\gamma})e^{-\gamma/\bar{\gamma}}$ [16], where $\bar{\gamma}$ is the average SNR. The instantaneous channel SNR is, $\gamma = |h|^2 P/\sigma^2$, where h is channel coefficient and σ^2 is noise power, while the average channel SNR is, $\bar{\gamma} = \varepsilon\{|h|^2\}P/\sigma^2$, where $\varepsilon\{\cdot\}$ denotes expectation. In addition, the normalized transmitted powers of the node A, relay and node B are, $P_A = 1$, $P_R = 1$, and $P_B = 1$, respectively, and the residual self-interference channels are assumed to be identical, i.e. $\bar{\gamma}_{AA} = \bar{\gamma}_{RR} = \bar{\gamma}_{BB} = \bar{\gamma}_{LI}$.

For FD-TWR, the relay simultaneously receives signals from both source nodes A and B, and the residual self-interference caused by its co-channel transmission signal, and then forwards them to the corresponding destination nodes B and A. The destination nodes B and A simultaneously receive signals forwarded by the relay, and residual self-interference created by their co-channel transmitted signals. In k-th time slot, the signals received at the relay, nodes B and A can be respectively expressed as

$$y_R[k] = h_{AR}x_A[k] + h_{BR}x_B[k] + h_{RR}t_R[k] + n_R[k], \quad (1)$$
$$y_B[k] = h_{RB}t_R[k] + h_{BB}t_B[k] + n_B[k], \quad (2)$$

and

$$y_A[k] = h_{RA}t_R[k] + h_{AA}t_A[k] + n_A[k], \quad (3)$$

where $t_R[k]$, $t_B[k]$, and $t_A[k]$ are the transmitted signals of the relay, nodes B and A, respectively.

III. Performance Analysis

A. Full-Duplex Two-Way Relaying With Amplify-and-Forward

The relay receives signals from both source nodes A and B, then forwards them to the corresponding destination nodes B and A, by amplifying the received signals based on the relaying channel gains. The destination nodes B and A simultaneously receive the signals, which are forwarded by the relay, and residual self-interference caused by their co-channel transmitted signals. Since both nodes B and A know their own transmitted symbols, they can perfectly subtract the back-propagating self-interference from the received signals before decoding, when node A, the relay, and node B have a perfect knowledge of the CSI.

Proposition 1: The instantaneous SNRs of the AF based FD-TWR at the nodes B and A can be respectively expressed as

$$\gamma_B = \frac{\gamma_{RB}\gamma_{AR}}{\gamma_{RB}(\bar{\gamma}_{RR}+1)+(\bar{\gamma}_{BB}+1)(\gamma_{AR}+\gamma_{BR}+\bar{\gamma}_{RR}+1)}, \tag{4}$$

and

$$\gamma_A = \frac{\gamma_{RA}\gamma_{BR}}{\gamma_{RA}(\bar{\gamma}_{RR}+1)+(\bar{\gamma}_{AA}+1)(\gamma_{AR}+\gamma_{BR}+\bar{\gamma}_{RR}+1)}. \tag{5}$$

Proof: See Appendix A. ■

Proposition 1 indicates that FD-TWR suffers from more severe residual self-interference compared to that in FD-OWR, because all the nodes in FD-TWR operate in full-duplex mode, while only the relay in FD-OWR operates in this mode. Thus, FD-TWR deteriorates the SNR of the received end-to-end signals.

According to [37, (20)], the average rate for the AF based FD-TWR is defined as

$$\begin{aligned}\bar{R} &= \varepsilon\{\log_2(1+\gamma_A)+\log_2(1+\gamma_B)\}\\ &= \varepsilon\{\log_2(1+\gamma_A)\}+\varepsilon\{\log_2(1+\gamma_B)\}.\end{aligned} \tag{6}$$

Different from the average rate for half-duplex relaying, the pre-log factor is 1 due to no spectral loss in FD operation.

Theorem 1: According to (4), (5), and (6), after solving the integral, the average rate for the AF based FD-TWR over Rayleigh fading channels is lower bounded as in (7), shown at the bottom of the page, where $E_1(x) = \int_1^\infty \frac{e^{-xt}}{t}dt$ [16].

Proof: See Appendix B. ■

For the AF based FD-OWR, the average rate over Rayleigh fading channel channels is given by [16], [22]

$$\bar{R}^{AF}_{FD-OWR} = \frac{\bar{\gamma}_{RB}(\bar{\gamma}_{RR}+1)e^{(\bar{\gamma}_{RR}+1)/\bar{\gamma}_{AR}}E_1\left(\frac{\bar{\gamma}_{RR}+1}{\bar{\gamma}_{AR}}\right)}{(\ln 2)(\bar{\gamma}_{RB}(\bar{\gamma}_{RR}+1)-\bar{\gamma}_{AR})} - \frac{\bar{\gamma}_{AR}e^{1/\bar{\gamma}_{RB}}E_1\left(\frac{1}{\bar{\gamma}_{RB}}\right)}{(\ln 2)(\bar{\gamma}_{RB}(\bar{\gamma}_{RR}+1)-\bar{\gamma}_{AR})}. \tag{8}$$

Note, that the lower bound in Theorem 1 is very tight in the medium to high SNR region. Furthermore, Theorem 1 indicates that the AF based FD-TWR cannot achieve full time multiplexing gain, compared with FD-OWR, because it also suffers from the residual self-interference at the two destination nodes.

For two-way relaying, both data streams must be successfully decoded at the destination nodes or else an outage will be declared. Let $\gamma_{th} = 2^{R_{th}}-1$, where γ_{th} and R_{th} are the outage SNR and rate thresholds, respectively. Thus, according to [37, (25) and (26)], the outage probability of FD-TWR is defined as

$$\begin{aligned}P^{AF}_{out}(R_{th}) &= P\{\min(\log_2(1+\gamma_A),\ \log_2(1+\gamma_B)) < R_{th}\}\\ &= P\{\min(\gamma_A,\ \gamma_B) < \gamma_{th}\}.\end{aligned} \tag{9}$$

Theorem 2: By substituting (4) and (5) into (9) and solving the double integral, the outage probability of the AF based FD-TWR can be tightly upper bounded by

$$\begin{aligned}P^{AF}_{out} \le{}& 1-2\left(\frac{\gamma_{th}(2\gamma_{th}+1)(\bar{\gamma}_{LI}+1)^2}{\bar{\gamma}_{AR}\bar{\gamma}_{BR}}\right)^{\frac{1}{2}}\\ &\times e^{-\frac{\gamma_{th}(\bar{\gamma}_{LI}+1)(2\bar{\gamma}_{AR}+\bar{\gamma}_{BR})}{\bar{\gamma}_{AR}\bar{\gamma}_{BR}}}K_1\left(2\left(\frac{\gamma_{th}(2\gamma_{th}+1)(\bar{\gamma}_{LI}+1)^2}{\bar{\gamma}_{AR}\bar{\gamma}_{BR}}\right)^{\frac{1}{2}}\right)\\ &+e^{-\frac{\gamma_{th}(\bar{\gamma}_{LI}+1)(2\bar{\gamma}_{AR}+\bar{\gamma}_{BR})}{\bar{\gamma}_{AR}\bar{\gamma}_{BR}}}\left(1-e^{-\frac{(\bar{\gamma}_{LI}+1)(\gamma_{th}+(9\gamma_{th}^2+4\gamma_{th})^{1/2})}{2\bar{\gamma}_{AR}}}\right)\\ &-e^{-\frac{\gamma_{th}(\bar{\gamma}_{LI}+1)(\bar{\gamma}_{AR}+2\bar{\gamma}_{BR})}{\bar{\gamma}_{AR}\bar{\gamma}_{BR}}}\left(1-e^{-\frac{(\bar{\gamma}_{LI}+1)(-\gamma_{th}+(9\gamma_{th}^2+4\gamma_{th})^{1/2})}{2\bar{\gamma}_{AR}}}\right),\end{aligned} \tag{10}$$

where $K_v(.)$ is the modified Bessel function of the second kind [22].

Proof: See Appendix C. ■

For the AF based FD-OWR, its outage probability is given by [22]

$$\begin{aligned}P^{AF,FD-OWR}_{out} ={}& 1-2\left(\frac{\gamma_{th}(\gamma_{th}+1)(\bar{\gamma}_{RR}+1)}{\bar{\gamma}_{AR}\bar{\gamma}_{RB}}\right)^{\frac{1}{2}}\\ &\times e^{-\frac{\gamma_{th}(\bar{\gamma}_{AR}+\bar{\gamma}_{RB}(\bar{\gamma}_{RR}+1))}{\bar{\gamma}_{AR}\bar{\gamma}_{RB}}}\\ &\times K_1\left(2\left(\frac{\gamma_{th}(\gamma_{th}+1)(\bar{\gamma}_{RR}+1)}{\bar{\gamma}_{AR}\bar{\gamma}_{RB}}\right)^{\frac{1}{2}}\right).\end{aligned} \tag{11}$$

The comparison of (10) in Theorem 2 and (11) indicates that the outage probability of the AF based FD-TWR is higher than that in FD-OWR. This is because the residual self-interference generated at the destination nodes in FD-TWR deteriorates the SNR of the received signals. Theorem 1 and Theorem 2 also reveal that time multiplexing can help to improve the average rate, but simultaneously it also leads to a loss in the outage performance.

B. Decode-and-Forward Based Full-Duplex Two-Way Relaying

1) Physical-Layer Network Coding: Physical-layer network coding applies bit-level XOR operation to two symbols

$$\begin{aligned}\bar{R}^{AF}_{sum} \ge{}& \frac{1}{\ln 2}\left(e^{\frac{2(\bar{\gamma}_{LI}+1)}{\bar{\gamma}_{BR}}}E_1\left(\frac{2(\bar{\gamma}_{LI}+1)}{\bar{\gamma}_{BR}}\right)+e^{\frac{2(\bar{\gamma}_{LI}+1)}{\bar{\gamma}_{AR}}}E_1\left(\frac{2(\bar{\gamma}_{LI}+1)}{\bar{\gamma}_{AR}}\right)\right.\\ &-\frac{\bar{\gamma}_{BR}}{2\bar{\gamma}_{RA}-\bar{\gamma}_{BR}}\left(e^{\frac{\bar{\gamma}_{LI}+1}{2\bar{\gamma}_{RA}}}E_1\left(\frac{\bar{\gamma}_{LI}+1}{2\bar{\gamma}_{RA}}\right)-e^{\frac{\bar{\gamma}_{LI}+1}{\bar{\gamma}_{BR}}}E_1\left(\frac{\bar{\gamma}_{LI}+1}{\bar{\gamma}_{BR}}\right)\right)\\ &\left.-\frac{\bar{\gamma}_{AR}}{2\bar{\gamma}_{RB}-\bar{\gamma}_{AR}}\left(e^{\frac{\bar{\gamma}_{LI}+1}{2\bar{\gamma}_{RB}}}E_1\left(\frac{\bar{\gamma}_{LI}+1}{2\bar{\gamma}_{RB}}\right)-e^{\frac{\bar{\gamma}_{LI}+1}{\bar{\gamma}_{AR}}}E_1\left(\frac{\bar{\gamma}_{LI}+1}{\bar{\gamma}_{AR}}\right)\right)\right)\end{aligned} \tag{7}$$

to generate a new symbol, then the network coded symbol can be transmitted with maximum power. For the DF based FD-TWR with PNC, the relay decodes the signals received from both source nodes A and B, then it implements PNC to recode the decoded data and forwards the recoded data to the destination nodes B and A. After receiving the network coded signals from the relay, the nodes B and A perform decoding to obtain their desired data, respectively. Since both nodes B and A know previously transmitted data, they can recover the desired data by using the same bit-level XOR operation.

Proposition 2: The instantaneous SNRs of the DF based FD-TWR with PNC at the relay, nodes B and A can be respectively expressed as

$$\gamma_R = \frac{\gamma_{AR} + \gamma_{BR}}{\bar{\gamma}_{RR} + 1}, \gamma_B = \frac{\gamma_{RB}}{\bar{\gamma}_{BB} + 1}, \gamma_A = \frac{\gamma_{RA}}{\bar{\gamma}_{AA} + 1}. \tag{12}$$

Proof: See Appendix D. ■

The average rate for the DF based full-duplex two-way relaying equals the average of the minimum of the rate for the source-relay and relay-destination channels, which is defined as [7][1]

$$\begin{aligned}\bar{R} = \varepsilon \Big\{ & \min(\log_2(1+\gamma_R), \\ & \min(\log_2(1+\gamma_{A2R}),\ \log_2(1+\gamma_{R2B})) \\ & + \min(\log_2(1+\gamma_{B2R}),\ \log_2(1+\gamma_{R2A}))) \Big\}. \end{aligned} \tag{13}$$

The pre-log factor is 1 due to no spectral loss in FD operation. Besides, unlike AF protocol, the rate for the DF based full-duplex two-way relaying is limited by both MAC and BC stages.

Theorem 3: According to (12) and (13) and applying Jensen's inequality, the average rate for the DF based FD-TWR with PNC can be upper bounded as in (14), shown at the bottom of the page.

Proof: See Appendix E. ■

[1]Note, that achieving the average rate, $\min(\varepsilon\{R_R\}, \varepsilon\{R_D\})$ [8], requires an idealistic setup with an infinite buffer at the relay, which can avoid overflows and underflows but suffer from large end-to-end delay.

According to [21, (5) and (6)], the average rate for the DF based FD-OWR can be expressed as

$$\bar{R} = \varepsilon\{\log_2(1 + \min(\gamma_R,\ \gamma_D))\}. \tag{15}$$

Considering Rayleigh fading channels and after solving the integral, its average rate can be written as

$$\begin{aligned}\bar{R} &= \varepsilon \left\{ \log_2 \left(1 + \min \left(\frac{\gamma_{AR}}{\bar{\gamma}_{RR}+1},\ \gamma_{RB} \right) \right) \right\} \\ &= \frac{1}{\ln 2} e^{\frac{(\bar{\gamma}_{AR} + \bar{\gamma}_{RB}(\bar{\gamma}_{RR}+1))}{\bar{\gamma}_{AR}\bar{\gamma}_{RB}}} E_1 \left(\frac{\bar{\gamma}_{AR} + \bar{\gamma}_{RB}(\bar{\gamma}_{RR}+1)}{\bar{\gamma}_{AR}\bar{\gamma}_{RB}} \right). \end{aligned} \tag{16}$$

Similar to [9, (14) and (15)], the outage probability of the DF based FD-TWR with PNC can be rewritten as

$$\begin{aligned} P_{out}^{DF} = 1 - P(\{ & \{\gamma_{A2R}^{DF} \ge \gamma_{th}\} \cap \{\gamma_{B2R}^{SIC} \ge \gamma_{th}\} \\ & \cap \{\gamma_{R2A}^{DF} \ge \gamma_{th}\} \cap \{\gamma_{R2B}^{DF} \ge \gamma_{th}\}\} \\ & \cup \{\{\gamma_{B2R}^{DF} \ge \gamma_{th}\} \cap \{\gamma_{A2R}^{SIC} \ge \gamma_{th}\} \\ & \cap \{\gamma_{R2A}^{DF} \ge \gamma_{th}\} \cap \{\gamma_{R2B}^{DF} \ge \gamma_{th}\}\}). \end{aligned} \tag{17}$$

Theorem 4: The outage probability of the DF based FD-TWR with PNC can be written as in (18), shown at the bottom of the page.

Proof: See Appendix A. ■

According to [24, (3)] and after solving the integral, a formula for the outage probability of the DF based FD-OWR under Rayleigh fading channels can be derived as

$$\begin{aligned} P_{out}^{DF} &= 1 - \left(1 - \int_0^{\gamma_{th}(\bar{\gamma}_{RR}+1)} \frac{1}{\bar{\gamma}_{AR}} e^{-x/\bar{\gamma}_{AR}} dx \right) \\ &\quad \times \left(1 - \int_0^{\gamma_{th}} \frac{1}{\bar{\gamma}_{RB}} e^{-y/\bar{\gamma}_{RB}} dy \right) \\ &= 1 - e^{-\frac{\gamma_{th}(\bar{\gamma}_{AR} + \bar{\gamma}_{RB}(\bar{\gamma}_{RR}+1))}{\bar{\gamma}_{AR}\bar{\gamma}_{RB}}}. \end{aligned} \tag{19}$$

The comparison of (18) and (19) reveals that the outage probability of the DF based FD-TWR with PNC is higher than that in the DF based FD-OWR, because residual self-interference, generated at the destination nodes due to their co-channel transmission, deteriorates the SNRs of the received signal.

$$\begin{aligned} \bar{R}_{sum}^{DF,PNC} \le \min \Bigg(& \frac{\bar{\gamma}_{BR} e^{\frac{\bar{\gamma}_{RR}+1}{\bar{\gamma}_{BR}}} E_1\left(\frac{\bar{\gamma}_{RR}+1}{\bar{\gamma}_{BR}}\right) - \bar{\gamma}_{AR} e^{\frac{\bar{\gamma}_{RR}+1}{\bar{\gamma}_{AR}}} E_1\left(\frac{\bar{\gamma}_{RR}+1}{\bar{\gamma}_{AR}}\right)}{(\ln 2)(\bar{\gamma}_{BR} - \bar{\gamma}_{AR})}, \\ & \frac{1}{\ln 2} e^{\frac{\bar{\gamma}_{AR}(\bar{\gamma}_{BB}+1) + \bar{\gamma}_{RB}(\bar{\gamma}_{RR}+1)}{\bar{\gamma}_{AR}\bar{\gamma}_{RB}}} E_1\left(\frac{\bar{\gamma}_{AR}(\bar{\gamma}_{BB}+1) + \bar{\gamma}_{RB}(\bar{\gamma}_{RR}+1)}{\bar{\gamma}_{AR}\bar{\gamma}_{RB}} \right) \\ & + \frac{1}{\ln 2} e^{\frac{\bar{\gamma}_{BR}(\bar{\gamma}_{AA}+1) + \bar{\gamma}_{RA}(\bar{\gamma}_{RR}+1)}{\bar{\gamma}_{BR}\bar{\gamma}_{RA}}} E_1\left(\frac{\bar{\gamma}_{BR}(\bar{\gamma}_{AA}+1) + \bar{\gamma}_{RA}(\bar{\gamma}_{RR}+1)}{\bar{\gamma}_{BR}\bar{\gamma}_{RA}} \right) \Bigg) \end{aligned} \tag{14}$$

$$P_{out}^{DF,PNC} = \begin{cases} 1 - \frac{\bar{\gamma}_{AR}}{\bar{\gamma}_{AR}+\bar{\gamma}_{BR}\gamma_{th}} e^{-\frac{\gamma_{th}(\bar{\gamma}_{LI}+1)(\bar{\gamma}_{AR}+\bar{\gamma}_{BR}+\bar{\gamma}_{BR}\gamma_{th})}{\bar{\gamma}_{AR}\bar{\gamma}_{BR}}} - \frac{\bar{\gamma}_{BR}}{\bar{\gamma}_{BR}+\bar{\gamma}_{AR}\gamma_{th}} e^{-\frac{\gamma_{th}(\bar{\gamma}_{LI}+1)(\bar{\gamma}_{AR}+\bar{\gamma}_{BR}+\bar{\gamma}_{AR}\gamma_{th})}{\bar{\gamma}_{AR}\bar{\gamma}_{BR}}}, & \gamma_{th} \ge 1 \\ 1 - \frac{\bar{\gamma}_{AR}}{\bar{\gamma}_{AR}+\bar{\gamma}_{BR}\gamma_{th}} e^{-\frac{\gamma_{th}(\bar{\gamma}_{LI}+1)(\bar{\gamma}_{AR}+\bar{\gamma}_{BR}+\bar{\gamma}_{BR}\gamma_{th})}{\bar{\gamma}_{AR}\bar{\gamma}_{BR}}} - \frac{\bar{\gamma}_{BR}}{\bar{\gamma}_{BR}+\bar{\gamma}_{AR}\gamma_{th}} e^{-\frac{\gamma_{th}(\bar{\gamma}_{LI}+1)(\bar{\gamma}_{AR}+\bar{\gamma}_{BR}+\bar{\gamma}_{AR}\gamma_{th})}{\bar{\gamma}_{AR}\bar{\gamma}_{BR}}} \\ + \frac{(1-\gamma_{th}^2)\bar{\gamma}_{AR}\bar{\gamma}_{BR}}{(\gamma_{th}\bar{\gamma}_{AR}+\bar{\gamma}_{BR})(\bar{\gamma}_{AR}+\gamma_{th}\bar{\gamma}_{BR})} e^{-\frac{\gamma_{th}(\bar{\gamma}_{LI}+1)(\bar{\gamma}_{AR}+\bar{\gamma}_{BR})}{(1-\gamma_{th})\bar{\gamma}_{AR}\bar{\gamma}_{BR}}}, & \gamma_{th} \in [0,\ 1) \end{cases} \tag{18}$$

2) Analog Network Coding: For ANC, the relay first decodes the signals received from source nodes A and B, then forwards the two data streams with power allocation factor $\theta \in (0, 1)$ and $1-\theta$, to the destination nodes B and A, respectively. The destination nodes B and A receive the mixed signal in power domain forwarded by the relay and residual self-interference caused by co-channel transmission, simultaneously. Since destination nodes know their previously transmitted data, they can subtract the back-propagating self-interference from the received signals before decoding. Note, that even if destination nodes do not have these prior data, they can also decode their desired data through successive interference cancellation (SIC).

Replacing γ_{RA} and γ_{RB} in (12) with $(1-\theta)\gamma_{RA}$ and $\theta\gamma_{RB}$, respectively, the instantaneous SNRs can be obtained from the corresponding PNC ones and are

$$\gamma_R = \frac{\gamma_{AR}+\gamma_{BR}}{\bar{\gamma}_{RR}+1}, \gamma_B = \frac{\theta\gamma_{RB}}{\bar{\gamma}_{BB}+1}, \gamma_A = \frac{(1-\theta)\gamma_{RA}}{\bar{\gamma}_{AA}+1}. \quad (20)$$

For ANC, the average rate for the DF based full-duplex two-way relaying can be further transformed into the following expression

$$\begin{aligned}\bar{R} = \varepsilon \Big\{ & \max_{\theta} \min(\log_2(1+\gamma_R), \\ & \min(\log_2(1+\gamma_{A2R}),\ \log_2(1+\gamma_{R2B})) \\ & + \min(\log_2(1+\gamma_{B2R}),\ \log_2(1+\gamma_{R2A})))\Big\}. \end{aligned} \quad (21)$$

Similar to the derivation of the average rate for PNC, combining (20) and (21), and applying Jensen's inequality, the average rate for the DF based FD-TWR with ANC can be upper bounded as in (22), shown at the bottom of the page.

Similar to the derivation of the outage probability of PNC, substituting (20) into (17), the outage probability of the DF based FD-TWR with ANC can be expressed as in (23), shown at the bottom of the page.

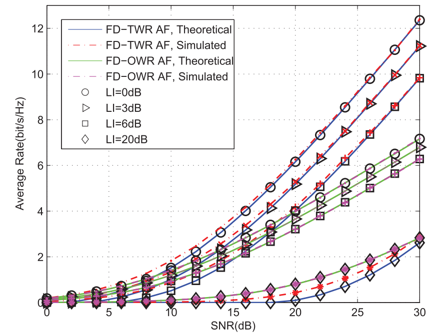

Fig. 2. Average rate for the AF based FD-OWR and FD-TWR.

IV. Numerical Results, Simulations, and Discussions

In this section, numerical results for the average rate and outage probability of FD-TWR scheme are presented and validated via Monte Carlo simulations.

Fig. 2 compares the average rate for the AF based FD-OWR and FD-TWR over Rayleigh fading channels. The results show that there is a cross point between the two curves. When the SNR is lower than the cross point, the average rate for the AF based FD-TWR is lower than that in the AF based FD-OWR, while higher rate for the AF based FD-TWR is achieved beyond the cross point. This is because the AF based FD-TWR can obtain time multiplexing gain by achieving bidirectional data transmission and reception between the nodes A and B via the relay in the same time slot, while FD-OWR needs two time slots to achieve that. However, since all the nodes work in full-duplex mode, it is inevitable that FD-TWR suffers from more severe residual self-interference than FD-OWR. The rate gain from time multiplexing cannot fully compensate for the loss in the rate, caused by the severe residual self-interference in the low SNR region.

$$\begin{aligned}\bar{R}_{sum}^{DF,ANC} \le \max_{\theta} \min \Bigg(& \frac{\bar{\gamma}_{BR} e^{\frac{\bar{\gamma}_{RR}+1}{\bar{\gamma}_{BR}}} E_1\left(\frac{\bar{\gamma}_{RR}+1}{\bar{\gamma}_{BR}}\right) - \bar{\gamma}_{AR} e^{\frac{\bar{\gamma}_{RR}+1}{\bar{\gamma}_{AR}}} E_1\left(\frac{\bar{\gamma}_{RR}+1}{\bar{\gamma}_{AR}}\right)}{(\ln 2)(\bar{\gamma}_{BR}-\bar{\gamma}_{AR})}, \\ & \frac{1}{\ln 2} e^{\frac{\bar{\gamma}_{AR}(\bar{\gamma}_{BB}+1)+\theta\bar{\gamma}_{RB}(\bar{\gamma}_{RR}+1)}{\theta\bar{\gamma}_{AR}\bar{\gamma}_{RB}}} E_1\left(\frac{\bar{\gamma}_{AR}(\bar{\gamma}_{BB}+1)+\theta\bar{\gamma}_{RB}(\bar{\gamma}_{RR}+1)}{\theta\bar{\gamma}_{AR}\bar{\gamma}_{RB}}\right) \\ & + \frac{1}{\ln 2} e^{\frac{\bar{\gamma}_{BR}(\bar{\gamma}_{AA}+1)+(1-\theta)\bar{\gamma}_{RA}(\bar{\gamma}_{RR}+1)}{(1-\theta)\bar{\gamma}_{BR}\bar{\gamma}_{RA}}} E_1\left(\frac{\bar{\gamma}_{BR}(\bar{\gamma}_{AA}+1)+(1-\theta)\bar{\gamma}_{RA}(\bar{\gamma}_{RR}+1)}{(1-\theta)\bar{\gamma}_{BR}\bar{\gamma}_{RA}}\right) \Bigg) \end{aligned} \quad (22)$$

$$P_{out}^{DF,ANC} = \begin{cases} 1 - \frac{\bar{\gamma}_{AR}}{\bar{\gamma}_{AR}+\bar{\gamma}_{BR}\gamma_{th}} e^{-\frac{\gamma_{th}(\bar{\gamma}_{LI}+1)(\bar{\gamma}_{AR}+\theta\bar{\gamma}_{BR}+\bar{\gamma}_{BR}\gamma_{th})}{\theta\bar{\gamma}_{AR}\bar{\gamma}_{BR}}} \\ -\frac{\bar{\gamma}_{BR}}{\bar{\gamma}_{BR}+\bar{\gamma}_{AR}\gamma_{th}} e^{-\frac{\gamma_{th}(\bar{\gamma}_{LI}+1)((1-\theta)\bar{\gamma}_{AR}+\bar{\gamma}_{BR}+\bar{\gamma}_{AR}\gamma_{th})}{(1-\theta)\bar{\gamma}_{AR}\bar{\gamma}_{BR}}}, & \gamma_{th} \ge 1 \\ 1 - \frac{\bar{\gamma}_{AR}}{\bar{\gamma}_{AR}+\bar{\gamma}_{BR}\gamma_{th}} e^{-\frac{\gamma_{th}(\bar{\gamma}_{LI}+1)(\bar{\gamma}_{AR}+\theta\bar{\gamma}_{BR}+\bar{\gamma}_{BR}\gamma_{th})}{\theta\bar{\gamma}_{AR}\bar{\gamma}_{BR}}} \\ -\frac{\bar{\gamma}_{BR}}{\bar{\gamma}_{BR}+\bar{\gamma}_{AR}\gamma_{th}} e^{-\frac{\gamma_{th}(\bar{\gamma}_{LI}+1)((1-\theta)\bar{\gamma}_{AR}+\bar{\gamma}_{BR}+\bar{\gamma}_{AR}\gamma_{th})}{(1-\theta)\bar{\gamma}_{AR}\bar{\gamma}_{BR}}} \\ +\frac{(1-\gamma_{th}^2)\bar{\gamma}_{AR}\bar{\gamma}_{BR}}{(\gamma_{th}\bar{\gamma}_{AR}+\bar{\gamma}_{BR})(\bar{\gamma}_{AR}+\gamma_{th}\bar{\gamma}_{BR})} e^{-\frac{\gamma_{th}(\bar{\gamma}_{LI}+1)(\bar{\gamma}_{AR}+\bar{\gamma}_{BR})}{(1-\gamma_{th})\bar{\gamma}_{AR}\bar{\gamma}_{BR}}}, & \gamma_{th} \in [0,\ 1) \textit{ and } \theta \in [1-\gamma_{th}, \gamma_{th}] \end{cases} \quad (23)$$

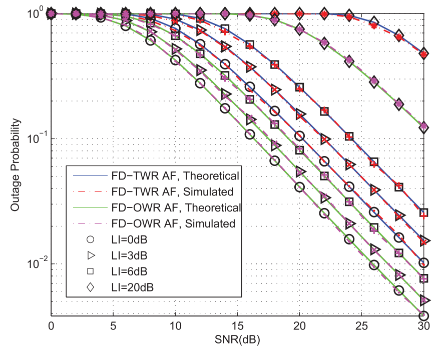

Fig. 3. Outage probability of the AF based FD-OWR and FD-TWR.

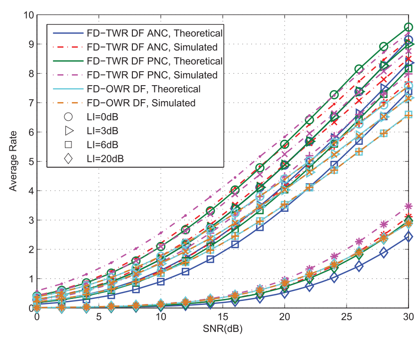

Fig. 4. Average rate for the DF based FD-OWR and FD-TWR.

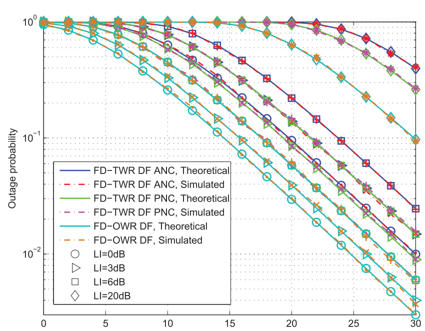

Fig. 5. Outage probability of the DF based FD-OWR and FD-TWR.

Fig. 3 depicts the outage probability of the AF based FD-OWR and FD-TWR over Rayleigh fading channels under the outage rate threshold, $R_{th} = 1$b/s/Hz. The results show that the outage probability of the AF based FD-TWR is higher than that in FD-OWR. This is because the AF based FD-TWR suffers from the residual self-interference not only at the relay but also at the destination nodes, which deteriorates the SNR of the end-to-end link.

Fig. 4 compares the average rate for the DF based FD-OWR and FD-TWR with PNC and ANC over Rayleigh fading channels. The results show that the DF based FD-TWR can achieve higher rate than FD-OWR. Besides, PNC can improve the rate for the DF based FD-TWR in the low SNR region, but it fails in the high SNRs because of the sum-rate limitation of the MAC stage.

Fig. 5 depicts the outage probability of the DF based FD-OWR and FD-TWR with PNC and ANC under the outage

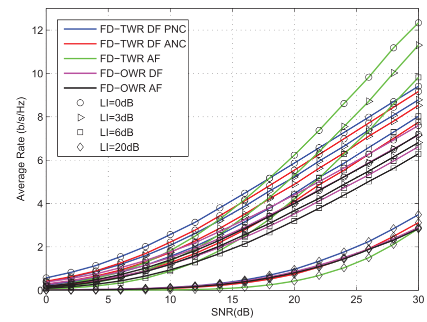

Fig. 6. Average rate for the FD-OWRs and FD-TWRs with different forwarding protocols and network coding schemes.

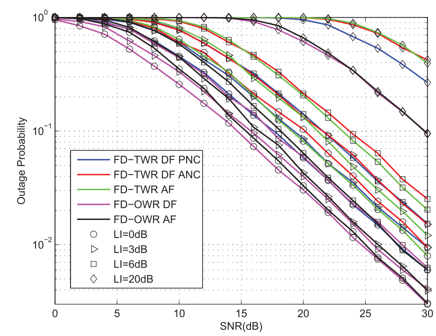

Fig. 7. Outage probability of the FD-OWRs and FD-TWRs with different forwarding protocols and network coding schemes.

rate threshold, $R_{th} = 1$b/s/Hz. The results show that the outage probability of the DF based FD-TWR is higher than that in FD-OWR, because the DF based FD-TWR suffers from more severe residual self-interference than FD-OWR. It is also shown that PNC can improve the outage performance of the DF based FD-TWR, because it enables the relay to forward the signals with maximum power without performing power allocation, which improves the quality of the relaying link.

In Fig. 6, a comparison is presented for the average rate for the FD-TWRs and FD-OWRs. It is obvious that there is a cross point between the AF and DF based FD-TWRs. When the SNR is lower than the cross point, the average rate for the DF based FD-TWR is better than that for the AF based FD-TWR. Conversely, the average rate for the DF based FD-TWR is lower than that for the AF based FD-TWR, when the SNR is higher than the cross point. It is also shown that the average rate for the DF based FD-TWR is better than that for the AF based FD-TWR, when there is strong residual self-interference. This is because AF protocol propagates residual self-interference, while DF protocol can suppress this propagation. Besides, the average rate for the DF based FD-TWR is limited by both MAC and BC stages, while AF protocol is not subjected to this limitation.

Fig. 7 depicts the outage probability of the FD-TWRs and FD-OWRs with different forwarding protocols and network coding schemes under the outage rate threshold, $R_{th} = 1$b/s/Hz. It can be observed that the outage probability of the DF based FD-TWR is lower than that in AF based FD-TWR, which is the same as above. It is also shown that the outage performance of the DF based FD-OWR is best, while the DF based FD-TWR with ANC is worst, followed by the AF based FD-OWR, the DF based FD-TWR with PNC, and the AF based FD-TWR. When residual self-interference is extremely severe, e.g. $LI \geq 30$ dB, the outage performance of the DF based FD-TWR with ANC is slightly better than that in the AF based FD-TWR.

V. CONCLUSIONS

The average rate and outage performance tradeoffs of two full-duplex relaying schemes, FD-OWR and FD-TWR based on AF and DF protocols, were investigated. Novel closed-form expressions for the average rate and outage probability of the second one, were derived. Furthermore, the application of network coding including PNC and ANC to full-duplex two-way relaying, was also studied. The effects of time multiplexing, network coding and forward protocol on relaying systems were analyzed, which would shed light on developing practical full-duplex relaying schemes. The results showed that there were tradeoffs of FD-OWR and FD-TWR under AF and DF protocols. FD-TWR achieves better average rate than that in FD-OWR, at the cost of a slight loss in the outage performance, when the residual self-interference was below a certain level, while DF protocol achieves better outage performance than that in AF protocol. However, it presents a slight loss in the rate in the high SNR region. In addition, DF protocol suppressed the residual self-interference propagation, but it was restricted to the rate achieved at both the MAC and BC stages, compared with AF protocol. The results also showed that PNC improves the rate and outage performance of the full-duplex two-way relaying. Therefore, in order to achieve better performance, it should dynamically switch to a proper relaying scheme, based on the quality of channels and residual self-interference. As it is assumed that the destination nodes in FD-TWR can perfectly subtract the back-propagating self-interference from the received signals before decoding, future work may further consider the effect of imperfect back-propagating self-interference subtraction.

APPENDIX A
PROOF OF PROPOSITION 1

For the AF based FD-TWR, in k-th time slot, the signal transmitted by the relay is the amplification of the prior received signal [16] and can be expressed as

$$\begin{aligned} t_R[k] &= \beta y_R[k-\tau] \\ &= \beta(h_{AR}x_A[k-\tau] + h_{BR}x_B[k-\tau] \\ &\quad + h_{RR}t_R[k-\tau] + n_R[k-\tau]), \end{aligned} \tag{24}$$

where β is the power amplification factor, which depends on the channel coefficients, and τ is the processing delay. Similarly to [30], the instantaneous transmitted power is expressed as

$$\begin{aligned} \varepsilon\{|t_R[k]|^2\} &= \beta^2(|h_{AR}|^2 + |h_{BR}|^2 + |h_{RR}|^2\varepsilon\{|t_R[k-\tau]|^2\} \\ &\quad + \sigma_R^2). \end{aligned} \tag{25}$$

Considering the power constraint of P_R at the relay and assuming that its average transmitted power is $\varepsilon\{|t_R[k]|^2\} = P_R = 1$, the amplification factor β can be determined from (25) as [34]

$$\beta = (|h_{AR}|^2 + |h_{BR}|^2 + |h_{RR}|^2 + \sigma_R^2)^{-\frac{1}{2}}, \tag{26}$$

where h_{RR} is residual self-interference after interference cancellation. By substituting (24) into (2), the received signal at the node B can be expressed as

$$\begin{aligned} y_B[k] &= h_{RB}(\beta y_R[k-\tau]) + h_{BB}t_B[k] + n_B[k] \\ &= \beta h_{RB}(h_{AR}x_A[k-\tau] + h_{BR}x_B[k-\tau] \\ &\quad + h_{RR}t_R[k-\tau] + n_R[k-\tau]) + h_{BB}t_B[k] + n_B[k]. \end{aligned} \tag{27}$$

Similarly to [16], since the node B know their own transmitted symbols, they can subtract the back-propagating self-interference in (27) before decoding, if perfect knowledge of the corresponding channel coefficients is assumed. The instantaneous powers of the signals received at these nodes are respectively expressed as

$$\begin{aligned} \varepsilon\{|y_B[k]|^2\} &= \beta^2|h_{RB}|^2(|h_{AR}|^2 + |h_{RR}|^2\varepsilon\{|t_R[k-\tau]|^2\} \\ &\quad + \sigma_R^2) + |h_{BB}|^2 + \sigma_B^2 \\ &= \beta^2|h_{RB}|^2(|h_{AR}|^2 + |h_{RR}|^2 + \sigma_R^2) + |h_{BB}|^2 \\ &\quad + \sigma_B^2. \end{aligned} \tag{28}$$

Therefore, the instantaneous SNR at the node B can be expressed as

$$\begin{aligned} \gamma_B &= \frac{\beta^2|h_{RB}|^2|h_{AR}|^2}{\beta^2|h_{RB}|^2(|h_{RR}|^2 + \sigma_R^2) + |h_{BB}|^2 + \sigma_B^2} \\ &= \frac{|h_{RB}|^2|h_{AR}|^2}{|h_{RB}|^2(|h_{RR}|^2 + \sigma_R^2) + \frac{|h_{BB}|^2 + \sigma_B^2}{\beta^2}}. \end{aligned} \tag{29}$$

Similarly, the instantaneous SNR at the node A can be expressed as

$$\begin{aligned} \gamma_A &= \frac{\beta^2|h_{RA}|^2|h_{BR}|^2}{\beta^2|h_{RA}|^2(|h_{RR}|^2 + \sigma_R^2) + |h_{AA}|^2 + \sigma_A^2} \\ &= \frac{|h_{RA}|^2|h_{BR}|^2}{|h_{RA}|^2(|h_{RR}|^2 + \sigma_R^2) + \frac{|h_{AA}|^2 + \sigma_A^2}{\beta^2}}. \end{aligned} \tag{30}$$

Finally, substituting (26) into (29) and (30), respectively, γ_B and γ_A are expressed as in (4) and (5) and the proof is completed.

APPENDIX B
PROOF OF THEOREM 1

Substituting (5) into (6), the average rate for the AF based FD-TWR achieved at the node A can be rewritten as in (31), shown at the bottom of the next page.

According to the assumption of identically residual self-interference, the double integral, $I_{1,1}$, can be simplified as in (32), shown at the bottom of the next page. In order to obtain a tightly lower bound easily, we discard the constant term $-(\bar{\gamma}_{LI} + 1)^2$ in the denominator. Then, the double integral, $I_{1,1}$, can be lower bounded as

$$
\begin{aligned}
I_{1,1} &> \int_0^\infty \int_0^\infty \frac{x+\bar{\gamma}_{LI}+1}{(x+\bar{\gamma}_{LI}+1)y+2(x+\bar{\gamma}_{LI}+1)(\bar{\gamma}_{LI}+1)} \\
&\quad \times \frac{1}{\bar{\gamma}_{RA}} e^{-\frac{x}{\bar{\gamma}_{RA}}} e^{-\frac{y}{\bar{\gamma}_{BR}}} dxdy \\
&= \int_0^\infty \int_0^\infty \frac{1}{y+2(\bar{\gamma}_{LI}+1)} \frac{1}{\bar{\gamma}_{RA}} e^{-\frac{x}{\bar{\gamma}_{RA}}} e^{-\frac{y}{\bar{\gamma}_{BR}}} dxdy \\
&= \int_0^\infty e^{\frac{2(\bar{\gamma}_{LI}+1)}{\bar{\gamma}_{BR}}} E_1\left(\frac{2(\bar{\gamma}_{LI}+1)}{\bar{\gamma}_{BR}}\right) \frac{1}{\bar{\gamma}_{RA}} e^{-\frac{x}{\bar{\gamma}_{RA}}} dx \\
&= e^{\frac{2(\bar{\gamma}_{LI}+1)}{\bar{\gamma}_{BR}}} E_1\left(\frac{2(\bar{\gamma}_{LI}+1)}{\bar{\gamma}_{BR}}\right)
\end{aligned} \tag{33}
$$

The double integral, $I_{1,2}$, can be solved as in (34), shown at the bottom of the page.

Substituting (33) and (34) into (31), the average rate for $B \to R \to A$ link is expressed as

$$
\begin{aligned}
\varepsilon\{\log_2(1+\gamma_A)\} &> \frac{1}{\ln 2}\left(e^{2(\bar{\gamma}_{LI}+1)/\bar{\gamma}_{BR}} E_1\left(\frac{2(\bar{\gamma}_{LI}+1)}{\bar{\gamma}_{BR}}\right)\right. \\
&\quad - \frac{\bar{\gamma}_{BR}}{2\bar{\gamma}_{RA}-\bar{\gamma}_{BR}}\left(e^{\frac{\bar{\gamma}_{LI}+1}{2\bar{\gamma}_{RA}}} E_1\left(\frac{\bar{\gamma}_{LI}+1}{2\bar{\gamma}_{RA}}\right)\right. \\
&\quad \left.\left. - e^{\frac{\bar{\gamma}_{LI}+1}{\bar{\gamma}_{BR}}} E_1\left(\frac{\bar{\gamma}_{LI}+1}{\bar{\gamma}_{BR}}\right)\right)\right).
\end{aligned} \tag{35}
$$

Similarly, the average rate for $A \to R \to B$ link is

$$
\begin{aligned}
\varepsilon\{\log_2(1+\gamma_B)\} &> \frac{1}{\ln 2}\left(e^{\frac{2(\bar{\gamma}_{LI}+1)}{\bar{\gamma}_{AR}}} E_1\left(\frac{2(\bar{\gamma}_{LI}+1)}{\bar{\gamma}_{AR}}\right)\right. \\
&\quad - \frac{\bar{\gamma}_{AR}}{2\bar{\gamma}_{RB}-\bar{\gamma}_{AR}}\left(e^{\frac{\bar{\gamma}_{LI}+1}{2\bar{\gamma}_{RB}}} E_1\left(\frac{\bar{\gamma}_{LI}+1}{2\bar{\gamma}_{RB}}\right)\right. \\
&\quad \left.\left. - e^{\frac{\bar{\gamma}_{LI}+1}{\bar{\gamma}_{AR}}} E_1\left(\frac{\bar{\gamma}_{LI}+1}{\bar{\gamma}_{AR}}\right)\right)\right).
\end{aligned} \tag{36}
$$

Finally, substituting (35) and (36) into (6), the average rate for the AF based FD-TWR is written as in (7) and the proof is completed.

Appendix C
Proof of Theorem 2

For the AF based FD-TWR, the integral domain for its outage probability consists of $D_1 = \{(x, y) | 0 < x < \infty, 0 < y \le \gamma_{th}(\bar{\gamma}_{LI}+1)\}$, $D_2 = \{(x, y) | 0 < x < \frac{\gamma_{th}(\bar{\gamma}_{LI}+1)(2y+(\bar{\gamma}_{LI}+1))}{y-\gamma_{th}(\bar{\gamma}_{LI}+1)}, \gamma_{th}(\bar{\gamma}_{LI}+1) < y < \infty\}$, and $D_3 = \{(x, y) | \frac{(\bar{\gamma}_{LI}+1)(3\gamma_{th}+(9\gamma_{th}^2+4\gamma_{th})^{1/2})}{2} \le x < \infty, \frac{\gamma_{th}(\bar{\gamma}_{LI}+1)(x+\bar{\gamma}_{LI}+1)}{x-2\gamma_{th}(\bar{\gamma}_{LI}+1)} \le y < \frac{\gamma_{th}(\bar{\gamma}_{LI}+1)(2x+\bar{\gamma}_{LI}+1)}{x-\gamma_{th}(\bar{\gamma}_{LI}+1)}\}$. Thus, the outage probability of the AF

$$
\begin{aligned}
&\varepsilon\{\log_2(1+\gamma_A)\} \\
&= \int_0^\infty \int_0^\infty \log_2\left(1+\frac{xy}{x(\bar{\gamma}_{RR}+1)+(\bar{\gamma}_{AA}+1)(x+y+\bar{\gamma}_{RR}+1)}\right) \frac{1}{\bar{\gamma}_{RA}} e^{-\frac{x}{\bar{\gamma}_{RA}}} \frac{1}{\bar{\gamma}_{BR}} e^{-\frac{y}{\bar{\gamma}_{BR}}} dxdy \\
&= \frac{1}{\ln 2}\left(\underbrace{\int_0^\infty \int_0^\infty \frac{x+\bar{\gamma}_{AA}+1}{xy+x(\bar{\gamma}_{RR}+1)+(\bar{\gamma}_{AA}+1)(x+y+\bar{\gamma}_{RR}+1)} \frac{1}{\bar{\gamma}_{RA}} e^{-\frac{x}{\bar{\gamma}_{RA}}} e^{-\frac{y}{\bar{\gamma}_{BR}}} dxdy}_{I_{1,1}}\right. \\
&\quad \left. - \underbrace{\int_0^\infty \int_0^\infty \frac{\bar{\gamma}_{AA}+1}{x(\bar{\gamma}_{RR}+1)+(\bar{\gamma}_{AA}+1)(x+y+\bar{\gamma}_{RR}+1)} \frac{1}{\bar{\gamma}_{RA}} e^{-\frac{x}{\bar{\gamma}_{RA}}} e^{-\frac{y}{\bar{\gamma}_{BR}}} dxdy}_{I_{1,2}}\right)
\end{aligned} \tag{31}
$$

$$
I_{1,1} = \int_0^\infty \int_0^\infty \frac{x+\bar{\gamma}_{LI}+1}{(x+\bar{\gamma}_{LI}+1)y+2(x+\bar{\gamma}_{LI}+1)(\bar{\gamma}_{LI}+1)-(\bar{\gamma}_{LI}+1)^2} \frac{1}{\bar{\gamma}_{RA}} e^{-\frac{x}{\bar{\gamma}_{RA}}} e^{-\frac{y}{\bar{\gamma}_{BR}}} dxdy \tag{32}
$$

$$
\begin{aligned}
I_{1,2} &= \int_0^\infty \int_0^\infty \frac{1}{\bar{\gamma}_{RA}} e^{-x/\bar{\gamma}_{RA}} e^{-y/\bar{\gamma}_{BR}} \frac{\bar{\gamma}_{AA}+1}{x(\bar{\gamma}_{RR}+1)+(\bar{\gamma}_{AA}+1)(x+y+\bar{\gamma}_{RR}+1)} dxdy \\
&= \int_0^\infty \int_0^\infty \frac{1}{\bar{\gamma}_{RA}} e^{-x/\bar{\gamma}_{RA}} e^{-y/\bar{\gamma}_{BR}} \frac{1}{y+2x+\bar{\gamma}_{LI}+1} dxdy \\
&= \frac{1}{\bar{\gamma}_{RA}} e^{(\bar{\gamma}_{LI}+1)/\bar{\gamma}_{BR}} \int_0^\infty e^{-x(1/\bar{\gamma}_{AR}-2/\bar{\gamma}_{BR})} E_1\left(\frac{2x+\bar{\gamma}_{LI}+1}{\bar{\gamma}_{BR}}\right) dx \\
&= \frac{\bar{\gamma}_{BR}}{2\bar{\gamma}_{RA}-\bar{\gamma}_{BR}}\left(e^{(\bar{\gamma}_{LI}+1)/(2\bar{\gamma}_{RA})} E_1\left(\frac{\bar{\gamma}_{LI}+1}{2\bar{\gamma}_{RA}}\right) - e^{(\bar{\gamma}_{LI}+1)/\bar{\gamma}_{BR}} E_1\left(\frac{\bar{\gamma}_{LI}+1}{\bar{\gamma}_{BR}}\right)\right).
\end{aligned} \tag{34}
$$

based FD-TWR can be derived as in (37), shown at the bottom of the page, where the first part, $I_{2,1}$, can be expressed as

$$I_{2,1} = 1 - \frac{1}{\bar{\gamma}_{BR}} \int_0^{\infty} e^{-\left(\frac{z}{\bar{\gamma}_{BR}} + \frac{\gamma_{th}(2\gamma_{th}+1)(\bar{\gamma}_{LI}+1)^2}{\bar{\gamma}_{AR} z}\right)} \times e^{-\frac{\gamma_{th}(\bar{\gamma}_{LI}+1)(\bar{\gamma}_{AR}+2\bar{\gamma}_{BR})}{\bar{\gamma}_{AR}\bar{\gamma}_{BR}}} dz$$
$$= 1 - 2\left(\frac{\gamma_{th}(2\gamma_{th}+1)(\bar{\gamma}_{LI}+1)^2}{\bar{\gamma}_{AR}\bar{\gamma}_{BR}}\right)^{\frac{1}{2}} \times e^{-\frac{\gamma_{th}(\bar{\gamma}_{LI}+1)(\bar{\gamma}_{AR}+2\bar{\gamma}_{BR})}{\bar{\gamma}_{AR}\bar{\gamma}_{BR}}} \times K_1\left(2\left(\frac{\gamma_{th}(2\gamma_{th}+1)(\bar{\gamma}_{LI}+1)^2}{\bar{\gamma}_{AR}\bar{\gamma}_{BR}}\right)^{\frac{1}{2}}\right), \quad (38)$$

and the second part, $I_{2,2}$, can be written as in (39), shown at the bottom of the page. When $\frac{(\bar{\gamma}_{LI}+1)(-\gamma_{th}+(9\gamma_{th}^2+4\gamma_{th})^{1/2})}{2}$ is very small, we ignore the item $\frac{\gamma_{th}(2\gamma_{th}+1)(\bar{\gamma}_{LI}+1)^2}{\bar{\gamma}_{BR} z}$. Therefore, $I_{2,2,1}$ can be expressed as

$$I_{2,2,1} < e^{-\frac{\gamma_{th}(\bar{\gamma}_{LI}+1)(\bar{\gamma}_{AR}+2\bar{\gamma}_{BR})}{\bar{\gamma}_{AR}\bar{\gamma}_{BR}}} \times \left(1 - e^{-\frac{(\bar{\gamma}_{LI}+1)(-\gamma_{th}+(9\gamma_{th}^2+4\gamma_{th})^{1/2})}{2\bar{\gamma}_{AR}}}\right). \quad (40)$$

Similarly, $I_{2,2,2}$ can be written as

$$I_{2,2,2} < e^{-\frac{\gamma_{th}(\bar{\gamma}_{LI}+1)(2\bar{\gamma}_{AR}+\bar{\gamma}_{BR})}{\bar{\gamma}_{AR}\bar{\gamma}_{BR}}} \times \left(1 - e^{-\frac{(\bar{\gamma}_{LI}+1)(\gamma_{th}+(9\gamma_{th}^2+4\gamma_{th})^{1/2})}{2\bar{\gamma}_{AR}}}\right). \quad (41)$$

Combining (37), (38), (39), (40), and (41), the tightly upper bound for the outage probability of the AF based FD-TWR can be expressed as (10), and the proof is completed.

$$P_{out}^{AF} = P(\min(\gamma_A, \gamma_B) < \gamma_{th}) = P(\{\gamma_A < \gamma_{th}\} \cup \{\gamma_B < \gamma_{th}\})$$
$$= \underbrace{\int_0^{\gamma_{th}(\bar{\gamma}_{LI}+1)} \frac{1}{\bar{\gamma}_{BR}} e^{-\frac{y}{\bar{\gamma}_{BR}}} \int_0^{\infty} \frac{1}{\bar{\gamma}_{AR}} e^{-\frac{x}{\bar{\gamma}_{AR}}} dx dy + \int_{\gamma_{th}(\bar{\gamma}_{LI}+1)}^{\infty} \frac{1}{\bar{\gamma}_{BR}} e^{-\frac{y}{\bar{\gamma}_{BR}}} \int_0^{\frac{\gamma_{th}(\bar{\gamma}_{LI}+1)(2y+(\bar{\gamma}_{LI}+1))}{y-\gamma_{th}(\bar{\gamma}_{LI}+1)}} \frac{1}{\bar{\gamma}_{AR}} e^{-\frac{x}{\bar{\gamma}_{AR}}} dx dy}_{I_{2,1}}$$
$$+ \underbrace{\int_{\frac{(\bar{\gamma}_{LI}+1)(3\gamma_{th}+(9\gamma_{th}^2+4\gamma_{th})^{1/2})}{2}}^{\infty} \int_{\frac{\gamma_{th}(\bar{\gamma}_{LI}+1)(x+\bar{\gamma}_{LI}+1)}{x-2\gamma_{th}(\bar{\gamma}_{LI}+1)}}^{\frac{\gamma_{th}(\bar{\gamma}_{LI}+1)(2x+\bar{\gamma}_{LI}+1)}{x-\gamma_{th}(\bar{\gamma}_{LI}+1)}} \frac{1}{\bar{\gamma}_{AR}} e^{-\frac{x}{\bar{\gamma}_{AR}}} \frac{1}{\bar{\gamma}_{BR}} e^{-\frac{y}{\bar{\gamma}_{BR}}} dx dy}_{I_{2,2}} \quad (37)$$

$$I_{2,2} = \frac{1}{\bar{\gamma}_{AR}} \int_{\frac{(\bar{\gamma}_{LI}+1)(-\gamma_{th}+(9\gamma_{th}^2+4\gamma_{th})^{1/2})}{2}}^{\infty} e^{-\left(\frac{z}{\bar{\gamma}_{AR}} + \frac{\gamma_{th}(2\gamma_{th}+1)(\bar{\gamma}_{LI}+1)^2}{\bar{\gamma}_{BR} z} + \frac{\gamma_{th}(\bar{\gamma}_{LI}+1)(\bar{\gamma}_{AR}+2\bar{\gamma}_{BR})}{\bar{\gamma}_{AR}\bar{\gamma}_{BR}}\right)} dz$$
$$- \frac{1}{\bar{\gamma}_{AR}} \int_{\frac{(\bar{\gamma}_{LI}+1)(\gamma_{th}+(9\gamma_{th}^2+4\gamma_{th})^{1/2})}{2}}^{\infty} e^{-\left(\frac{z}{\bar{\gamma}_{AR}} + \frac{\gamma_{th}(2\gamma_{th}+1)(\bar{\gamma}_{LI}+1)^2}{\bar{\gamma}_{BR} z} + \frac{\gamma_{th}(\bar{\gamma}_{LI}+1)(2\bar{\gamma}_{AR}+\bar{\gamma}_{BR})}{\bar{\gamma}_{AR}\bar{\gamma}_{BR}}\right)} dz$$
$$= 2\left(\frac{\gamma_{th}(2\gamma_{th}+1)(\bar{\gamma}_{LI}+1)^2}{\bar{\gamma}_{AR}\bar{\gamma}_{BR}}\right)^{\frac{1}{2}} e^{-\frac{\gamma_{th}(\bar{\gamma}_{LI}+1)(\bar{\gamma}_{AR}+2\bar{\gamma}_{BR})}{\bar{\gamma}_{AR}\bar{\gamma}_{BR}}} K_1\left(2\left(\frac{\gamma_{th}(2\gamma_{th}+1)(\bar{\gamma}_{LI}+1)^2}{\bar{\gamma}_{AR}\bar{\gamma}_{BR}}\right)^{\frac{1}{2}}\right)$$
$$\underbrace{- \frac{1}{\bar{\gamma}_{AR}} \int_0^{\frac{(\bar{\gamma}_{LI}+1)(-\gamma_{th}+(9\gamma_{th}^2+4\gamma_{th})^{1/2})}{2}} e^{-\left(\frac{z}{\bar{\gamma}_{AR}} + \frac{\gamma_{th}(2\gamma_{th}+1)(\bar{\gamma}_{LI}+1)^2}{\bar{\gamma}_{BR} z} + \frac{\gamma_{th}(\bar{\gamma}_{LI}+1)(\bar{\gamma}_{AR}+2\bar{\gamma}_{BR})}{\bar{\gamma}_{AR}\bar{\gamma}_{BR}}\right)} dz}_{I_{2,2,1}}$$
$$- 2\left(\frac{\gamma_{th}(2\gamma_{th}+1)(\bar{\gamma}_{LI}+1)^2}{\bar{\gamma}_{AR}\bar{\gamma}_{BR}}\right)^{\frac{1}{2}} e^{-\frac{\gamma_{th}(\bar{\gamma}_{LI}+1)(2\bar{\gamma}_{AR}+\bar{\gamma}_{BR})}{\bar{\gamma}_{AR}\bar{\gamma}_{BR}}} K_1\left(2\left(\frac{\gamma_{th}(2\gamma_{th}+1)(\bar{\gamma}_{LI}+1)^2}{\bar{\gamma}_{AR}\bar{\gamma}_{BR}}\right)^{\frac{1}{2}}\right)$$
$$+ \underbrace{\frac{1}{\bar{\gamma}_{AR}} \int_0^{\frac{(\bar{\gamma}_{LI}+1)(\gamma_{th}+(9\gamma_{th}^2+4\gamma_{th})^{1/2})}{2}} e^{-\left(\frac{z}{\bar{\gamma}_{AR}} + \frac{\gamma_{th}(2\gamma_{th}+1)(\bar{\gamma}_{LI}+1)^2}{\bar{\gamma}_{BR} z} + \frac{\gamma_{th}(\bar{\gamma}_{LI}+1)(2\bar{\gamma}_{AR}+\bar{\gamma}_{BR})}{\bar{\gamma}_{AR}\bar{\gamma}_{BR}}\right)} dz}_{I_{2,2,2}} \quad (39)$$

Appendix D
Proof of Proposition 2

For the DF based FD-TWR with PNC, in k-th time slot, the signal transmitted at the relay can be expressed as

$$t_R[k] = x_A[k-\tau] \oplus x_B[k-\tau]. \tag{42}$$

According to (1), the instantaneous SNR of the signal received at the relay is expressed as

$$\gamma_R = \frac{\varepsilon\{|h_{AR}x_A[k]|^2\} + \varepsilon\{|h_{BR}x_B[k]|^2\}}{\varepsilon\{|h_{RR}t_R[k]|^2\} + \varepsilon\{|n_R[k]|^2\}} = \frac{\gamma_{AR}+\gamma_{BR}}{\bar{\gamma}_{RR}+1}. \tag{43}$$

Substituting (42) into (2) and (3), it holds that

$$y_B[k] = h_{RB}(x_A[k-\tau] \oplus x_B[k-\tau]) + h_{BB}t_B[k] + n_B[k], \tag{44}$$

and

$$y_A[k] = h_{RA}(x_A[k-\tau] \oplus x_B[k-\tau]) + h_{AA}t_A[k] + n_A[k]. \tag{45}$$

Since both destination nodes B and A know their preciously transmitted data, they can subtract the back-propagating self-interference in (44) and (45) after decoding, through bit-level XOR operation. The instantaneous SNRs of signals received at nodes B and A can be respectively expressed as

$$\gamma_B = \frac{\varepsilon\{|h_{RB}x_A[k-\tau]|^2\}}{\varepsilon\{|h_{BB}t_B[k]|^2\} + \varepsilon\{|n_B[k]|^2\}} = \frac{\gamma_{RB}}{\bar{\gamma}_{BB}+1}, \tag{46}$$

and

$$\gamma_A = \frac{\varepsilon\{|h_{RA}x_B[k-\tau]|^2\}}{\varepsilon\{|h_{AA}t_A[k]|^2\} + \varepsilon\{|n_A[k]|^2\}} = \frac{\gamma_{RA}}{\bar{\gamma}_{AA}+1}, \tag{47}$$

and Proposition 2 is proved.

Appendix E
Proof of Theorem 3

Applying Jensen's inequality to (13), the average rate for the DF based FD-TWR with PNC over Rayleigh fading channels is upper bounded as

$$\begin{aligned}\bar{R} \le \min\big(&\varepsilon\{\log_2(1+\gamma_R)\},\ \varepsilon\{\log_2(1+\min(\gamma_{A2R},\ \gamma_{R2B}))\} \\ &+\varepsilon\{\log_2(1+\min(\gamma_{B2R},\ \gamma_{R2A}))\}\big),\end{aligned} \tag{48}$$

where $\varepsilon\{\log_2(1+\gamma_R)\}$ is expressed as in (49), shown at the bottom of the page.

In order to derive the closed-form-expression conveniently, we first define a random variable X as the minimum of γ_{A2R} and γ_{R2B}, namely $X = \min(\gamma_{A2R}, \gamma_{R2B}) =$

$$\begin{aligned}
\varepsilon\{\log_2(1+\gamma_R)\} &= \varepsilon\left\{\log_2\left(1+\frac{\gamma_{AR}+\gamma_{BR}}{\bar{\gamma}_{RR}+1}\right)\right\} \\
&= \int_0^\infty\int_0^\infty \log_2\left(1+\frac{x+y}{\bar{\gamma}_{RR}+1}\right)\frac{1}{\bar{\gamma}_{AR}}e^{-x/\bar{\gamma}_{AR}}\frac{1}{\bar{\gamma}_{BR}}e^{-y/\bar{\gamma}_{BR}}dxdy \\
&= \frac{1}{\ln 2}\int_0^\infty \frac{e^{-y/\bar{\gamma}_{BR}}}{\bar{\gamma}_{BR}}\left\{\left[-e^{-x/\bar{\gamma}_{AR}}\ln\left(1+\frac{x+y}{\bar{\gamma}_{RR}+1}\right)\right]_0^\infty + \int_0^\infty \frac{1}{\bar{\gamma}_{RR}+1+x+y}e^{-x/\bar{\gamma}_{AR}}dx\right\}dy \\
&= \frac{1}{\ln 2}\left\{\int_0^\infty \ln\left(1+\frac{y}{\bar{\gamma}_{RR}+1}\right)\frac{e^{-y/\bar{\gamma}_{BR}}}{\bar{\gamma}_{BR}}dy + \int_0^\infty\int_0^\infty \frac{1}{\bar{\gamma}_{RR}+1+x+y}e^{-x/\bar{\gamma}_{AR}}\frac{e^{-y/\bar{\gamma}_{BR}}}{\bar{\gamma}_{BR}}dxdy\right\} \\
&= \begin{cases} \frac{1}{\ln 2}\left(1+\frac{(\bar{\gamma}_{BR}-(\bar{\gamma}_{RR}+1))e^{(\bar{\gamma}_{RR}+1)/\bar{\gamma}_{BR}}E_1\left(\frac{\bar{\gamma}_{RR}+1}{\bar{\gamma}_{BR}}\right)}{\bar{\gamma}_{BR}}\right), & \bar{\gamma}_{BR}=\bar{\gamma}_{AR} \\ \frac{\bar{\gamma}_{BR}e^{(\bar{\gamma}_{RR}+1)/\bar{\gamma}_{BR}}E_1\left(\frac{\bar{\gamma}_{RR}+1}{\bar{\gamma}_{BR}}\right)-\bar{\gamma}_{AR}e^{(\bar{\gamma}_{RR}+1)/\bar{\gamma}_{AR}}E_1\left(\frac{\bar{\gamma}_{RR}+1}{\bar{\gamma}_{AR}}\right)}{(\ln 2)(\bar{\gamma}_{BR}-\bar{\gamma}_{AR})}, & \bar{\gamma}_{BR}\neq\bar{\gamma}_{AR}\end{cases}
\end{aligned} \tag{49}$$

$$\begin{aligned}
P_{out}^{DF,PNC} &= 1 - \int_{\gamma_{th}(\bar{\gamma}_{LI}+1)}^\infty\int_{\gamma_{th}(y+\bar{\gamma}_{LI}+1)}^\infty \frac{1}{\bar{\gamma}_{AR}}e^{-x/\bar{\gamma}_{AR}}\frac{1}{\bar{\gamma}_{BR}}e^{-y/\bar{\gamma}_{BR}}dxdy \\
&\quad - \int_{\gamma_{th}(\bar{\gamma}_{LI}+1)}^\infty\int_{\gamma_{th}(x+\bar{\gamma}_{LI}+1)}^\infty \frac{1}{\bar{\gamma}_{AR}}e^{-x/\bar{\gamma}_{AR}}\frac{1}{\bar{\gamma}_{BR}}e^{-y/\bar{\gamma}_{BR}}dxdy \\
&\quad + \int_{\gamma_{th}(\bar{\gamma}_{LI}+1)/(1-\gamma_{th})}^\infty\int_{\gamma_{th}(x+\bar{\gamma}_{LI}+1)}^{x/\gamma_{th}-(\bar{\gamma}_{LI}+1)} \frac{1}{\bar{\gamma}_{AR}}e^{-x/\bar{\gamma}_{AR}}\frac{1}{\bar{\gamma}_{BR}}e^{-y/\bar{\gamma}_{BR}}dxdy \\
&= 1 - \frac{\bar{\gamma}_{AR}}{\bar{\gamma}_{AR}+\bar{\gamma}_{BR}\gamma_{th}}e^{-\frac{\gamma_{th}(\bar{\gamma}_{LI}+1)(\bar{\gamma}_{AR}+\bar{\gamma}_{BR}+\bar{\gamma}_{BR}\gamma_{th})}{\bar{\gamma}_{AR}\bar{\gamma}_{BR}}} - \frac{\bar{\gamma}_{BR}}{\bar{\gamma}_{BR}+\bar{\gamma}_{AR}\gamma_{th}}e^{-\frac{\gamma_{th}(\bar{\gamma}_{LI}+1)(\bar{\gamma}_{AR}+\bar{\gamma}_{BR}+\bar{\gamma}_{AR}\gamma_{th})}{\bar{\gamma}_{AR}\bar{\gamma}_{BR}}} \\
&\quad + \frac{(1-\gamma_{th}^2)\bar{\gamma}_{AR}\bar{\gamma}_{BR}}{(\gamma_{th}\bar{\gamma}_{AR}+\bar{\gamma}_{BR})(\bar{\gamma}_{AR}+\gamma_{th}\bar{\gamma}_{BR})}e^{-\frac{\gamma_{th}(\bar{\gamma}_{LI}+1)(\bar{\gamma}_{AR}+\bar{\gamma}_{BR})}{(1-\gamma_{th})\bar{\gamma}_{AR}\bar{\gamma}_{BR}}}
\end{aligned} \tag{55}$$

$\min\left(\frac{\gamma_{AR}}{\bar{\gamma}_{RR}+1},\ \frac{\gamma_{RB}}{\bar{\gamma}_{BB}+1}\right)$. Then, we deduce its cumulative distribution function (CDF) as below

$$\begin{aligned} F_X(x) &= P(X \le x) = P(\min(\gamma_{A2R}, \gamma_{R2B}) \le x) \\ &= F_{\gamma_{A2R}}(x) + F_{\gamma_{R2B}}(x) - F_{\gamma_{A2R}}(x)F_{\gamma_{R2B}}(x) \\ &= \begin{cases} 1 - e^{-\frac{(\bar{\gamma}_{AR}(\bar{\gamma}_{BB}+1)+\bar{\gamma}_{RB}(\bar{\gamma}_{RR}+1))x}{\bar{\gamma}_{AR}\bar{\gamma}_{RB}}}, & x > 0 \\ 0, & x \le 0. \end{cases} \end{aligned} \tag{50}$$

Based on CDF of X, $\varepsilon\{\log_2(1+\min(\gamma_{A2R},\ \gamma_{R2B}))\}$ is derived as below

$$\begin{aligned} \bar{R}_B^{DF} &= \varepsilon\{\log_2(1+\min(\gamma_{A2R},\ \gamma_{R2B}))\} \\ &= \int_0^\infty \log_2(1+x)dF_X(x) \\ &= \int_0^\infty \log_2(1+x)\frac{\bar{\gamma}_{AR}(\bar{\gamma}_{BB}+1)+\bar{\gamma}_{RB}(\bar{\gamma}_{RR}+1)}{\bar{\gamma}_{AR}\bar{\gamma}_{RB}} \\ &\quad \times e^{-\frac{(\bar{\gamma}_{AR}(\bar{\gamma}_{BB}+1)+\bar{\gamma}_{RB}(\bar{\gamma}_{RR}+1))x}{\bar{\gamma}_{AR}\bar{\gamma}_{RB}}}dx \\ &= \frac{1}{\ln 2}\int_0^\infty \frac{1}{1+x}e^{-\frac{(\bar{\gamma}_{AR}(\bar{\gamma}_{BB}+1)+\bar{\gamma}_{RB}(\bar{\gamma}_{RR}+1))x}{\bar{\gamma}_{AR}\bar{\gamma}_{RB}}}dx \\ &= \frac{1}{\ln 2}e^{\frac{\bar{\gamma}_{AR}(\bar{\gamma}_{BB}+1)+\bar{\gamma}_{RB}(\bar{\gamma}_{RR}+1)}{\bar{\gamma}_{AR}\bar{\gamma}_{RB}}} \\ &\quad \times E_1\left(\frac{\bar{\gamma}_{AR}(\bar{\gamma}_{BB}+1)+\bar{\gamma}_{RB}(\bar{\gamma}_{RR}+1)}{\bar{\gamma}_{AR}\bar{\gamma}_{RB}}\right). \end{aligned} \tag{51}$$

Similarly, $\varepsilon\{\log_2(1+\min(\gamma_{B2R},\ \gamma_{R2A}))\}$ can be expressed as

$$\begin{aligned} \bar{R}_A^{DF} &= \varepsilon\{\log_2(1+\min(\gamma_{B2R},\ \gamma_{R2A}))\} \\ &= \frac{1}{\ln 2}e^{\frac{\bar{\gamma}_{BR}(\bar{\gamma}_{AA}+1)+\bar{\gamma}_{RA}(\bar{\gamma}_{RR}+1)}{\bar{\gamma}_{BR}\bar{\gamma}_{RA}}} \\ &\quad \times E_1\left(\frac{\bar{\gamma}_{BR}(\bar{\gamma}_{AA}+1)+\bar{\gamma}_{RA}(\bar{\gamma}_{RR}+1)}{\bar{\gamma}_{BR}\bar{\gamma}_{RA}}\right). \end{aligned} \tag{52}$$

Substituting (49), (51) and (52) into (48), the average rate for the DF based FD-TWR with PNC is written as in (14) and the proof is completed.

Appendix F
Proof of Theorem 4

For the instantaneous data transmission of the DF based FD-TWR with PNC, we have

$$\begin{aligned} \gamma_{A2R}^{DF} &= \frac{\gamma_{AR}}{\gamma_{BR}+\bar{\gamma}_{RR}+1},\ \gamma_{A2R}^{SIC} = \frac{\gamma_{AR}}{\bar{\gamma}_{RR}+1}, \\ \gamma_{B2R}^{DF} &= \frac{\gamma_{BR}}{\gamma_{AR}+\bar{\gamma}_{RR}+1},\ \gamma_{B2R}^{SIC} = \frac{\gamma_{BR}}{\bar{\gamma}_{RR}+1}, \\ \gamma_{R2A}^{DF} &= \frac{\gamma_{RA}}{\bar{\gamma}_{AA}+1},\ \gamma_{R2B}^{DF} = \frac{\gamma_{RB}}{\bar{\gamma}_{BB}+1}. \end{aligned} \tag{53}$$

Under the condition of the channels' reciprocal property and identical self-interference assumption, by combining (17) and (53), the outage probability of the DF based FD-TWR with PNC can be derived as follow:

Case 1: when $\gamma_{th} \ge 1$, the integrating range is not overlapped. After solving the double integral, the expression for the outage probability can be obtained and is

$$\begin{aligned} P_{out}^{DF,PNC} &= 1 - \int_{\gamma_{th}(\bar{\gamma}_{LI}+1)}^\infty \int_{\gamma_{th}(y+\bar{\gamma}_{LI}+1)}^\infty \frac{1}{\bar{\gamma}_{AR}}e^{-x/\bar{\gamma}_{AR}} \\ &\quad \times \frac{1}{\bar{\gamma}_{BR}}e^{-y/\bar{\gamma}_{BR}}dxdy \\ &\quad - \int_{\gamma_{th}(\bar{\gamma}_{LI}+1)}^\infty \int_{\gamma_{th}(x+\bar{\gamma}_{LI}+1)}^\infty \frac{1}{\bar{\gamma}_{AR}}e^{-x/\bar{\gamma}_{AR}} \\ &\quad \times \frac{1}{\bar{\gamma}_{BR}}e^{-y/\bar{\gamma}_{BR}}dxdy \\ &= 1 - \frac{\bar{\gamma}_{AR}}{\bar{\gamma}_{AR}+\bar{\gamma}_{BR}\gamma_{th}}e^{-\frac{\gamma_{th}(\bar{\gamma}_{LI}+1)(\bar{\gamma}_{AR}+\bar{\gamma}_{BR}+\bar{\gamma}_{BR}\gamma_{th})}{\bar{\gamma}_{AR}\bar{\gamma}_{BR}}} \\ &\quad - \frac{\bar{\gamma}_{BR}}{\bar{\gamma}_{BR}+\bar{\gamma}_{AR}\gamma_{th}}e^{-\frac{\gamma_{th}(\bar{\gamma}_{LI}+1)(\bar{\gamma}_{AR}+\bar{\gamma}_{BR}+\bar{\gamma}_{AR}\gamma_{th})}{\bar{\gamma}_{AR}\bar{\gamma}_{BR}}}. \end{aligned} \tag{54}$$

Case 2: when $\gamma_{th} \in [0,\ 1)$, there is overlapped integrating area. Through solving the double integral, we obtain the expression for the outage probability as in (55) at the bottom of the previous page.

Therefore, the outage probability of the DF based FD-TWR with PNC can be written as in (18), and the proof is completed.

References

[1] J. I. Choiy, M. Jainy, K. Srinivasany, P. Levis, and S. Katti, "Achieving single channel, full duplex wireless communication," in *Proc. ACM MobiCom*, 2010, pp. 1–12.

[2] M. Duarte, C. Dick, and A. Sabharwal, "Experiment-driven characterization of full-duplex wireless systems," *IEEE Trans. Wireless Commun.*, vol. 11, no. 12, pp. 4296–4307, Dec. 2012.

[3] D. Bharadia, E. McMilin, and S. Katti, "Full-duplex radios," in *Proc. ACM SIGCOMM*, 2013, pp. 375–386.

[4] B. Debaillie *et al.*, "Analog/RF solutions enabling compact full-duplex radios," *IEEE J. Sel. Areas Commun.*, vol. 32, no. 9, pp. 1662–1673, Sep. 2014.

[5] A. Cirik *et al.*, "Radio resource management and protocol solutions for full-duplex systems," DUPLO Deliverable D4.2, Project Number 316369, 22 May, 2015 [Online]. Available: http://www.fp7-duplo.eu/index.php/deliverables.

[6] Z. Zhang, X. Chai, K. Long, A. V. Vasilakos, and L. Hanzo, "Full duplex techniques for 5G networks: Self-interference cancellation, protocol design, and relay selection," *IEEE Commun. Mag.*, vol. 53, no. 5, pp. 128–137, May 2015.

[7] B. Rankov and A. Wittneben, "Spectral efficient protocols for half-duplex fading relay channels," *IEEE J. Sel. Areas Commun.*, vol. 25, no. 2, pp. 379–389, Feb. 2007.

[8] B. Xia, Y. Fan, J. Thompson, and H. V. Poor, "Buffering in a three-node relay network," *IEEE Trans. Wireless Commun.*, vol. 7, no. 11, pp. 4492–4496, Nov. 2008.

[9] Q. Li, S. Ting, A. Pandharipande, and Y. Han, "Adaptive two-way relaying and outage analysis," *IEEE Trans. Commun.*, vol. 8, no. 6, pp. 3288–3299, Jun. 2009.

[10] T. Q. Duong, V. N. Q. Bao, and H. Zepernick, "On the performance of selection decode-and-forward relay networks over Nakagami-m fading channels," *IEEE Commun. Lett.*, vol. 13, no. 3, pp. 172–174, Mar. 2009.

[11] M. Elkashlan, P. L. Yeoh, R. H. Y. Louie, and I. B. Collings, "On the exact and asymptotic SER of receive diversity with multiple amplify-and-forward relays," *IEEE Trans. Veh. Technol.*, vol. 59, no. 9, pp. 4602–4608, Nov. 2010.

[12] C. Zhong, S. Jin, and K. Wong, "Dual-hop systems with noisy relay and interference-limited destination," *IEEE Trans. Commun.*, vol. 58, no. 3, pp. 764–768, Mar. 2010.

[13] D. B. da Costa and M. D. Yacoub, "Outage performance of two hop AF relaying systems with co-channel interferers over Nakagami-m fading," *IEEE Commun. Lett.*, vol. 15, no. 9, pp. 980–982, Sep. 2011.

[14] Relay Radio Transmission and Reception, 3GPP TR 36.826, Jul. 2013.

[15] Relay Architectures for E-UTRA (LTE-Advanced), 3GPP TR 36.806, Mar. 2010.

[16] T. Riihonen, S. Werner, and R. Wichman, "Comparison of full-duplex and half-duplex modes with a fixed amplify-and-forward relay," in *Proc. IEEE Wireless Commun. Netw. Conf. (WCNC)*, 2009, pp. 1–5.

[17] B. Rankov and A. Wittneben, "Achievable rate regions for the two-way relay channel," in *Proc. IEEE Int. Symp. Inf. Theory (ISIT)*, 2006, pp. 1668–1672.

[18] H. Ju, E. Oh, and D. Hong, "Catching resource-devouring worms in next-generation wireless relay systems: Two-way relay and full-duplex relay," *IEEE Commun. Mag.*, vol. 47, no. 9, pp. 58–65, Sep. 2009.

[19] R. H. Y. Louie, Y. Li, and B. Vucetic, "Practical physical layer network coding for two-way relay channels: Performance analysis and comparison," *IEEE Trans. Wireless Commun.*, vol. 9, no. 2, pp. 764–777, Feb. 2010.

[20] S. Katti, S. Gollakota, and D. Katabi, "Embracing wireless interference: Analog network coding," in *Proc. ACM SIGCOMM*, 2007, pp. 27–31.

[21] T. Riihonen, S. Werner, and R. Wichman, "Rate-interference trade-off between duplex modes in decode-and-forward relaying," in *Proc. IEEE 21st Int. Symp. Pers. Indoor Mobile Radio Commun. (PIMRC)*, 2010, pp. 690–695.

[22] R. Hu, C. Hu, J. Jiang, X. Xie, and L. Song, "Full-duplex mode in amplify-and-forward relay channels: Outage probability and ergodic capacity," *Int. J. Antennas Propag.*, vol. 31, no. 1, pp. 1–8, 2014.

[23] T. Riihonen, S. Werner, and R. Wichman, "Optimized gain control for single-frequency relaying with loop interference," *IEEE Trans. Wireless Commun.*, vol. 8, no. 6, pp. 2801–2806, Jun. 2009.

[24] T. Kwon, S. Lim, S. Choi, and D. Hong, "Optimal duplex mode for DF relay in terms of the outage probability," *IEEE Trans. Veh. Technol.*, vol. 59, no. 7, pp. 3628–3634, Sep. 2010.

[25] B. P. Day, A. R. Margetts, D. W. Bliss, and P. Schniter, "Full-duplex MIMO relaying: Achievable rates under limited dynamic range," *IEEE J. Sel. Areas Commun.*, vol. 30, no. 8, pp. 1541–1553, Sep. 2012.

[26] T. Riihonen, S. Werner, and R. Wichman, "Hybrid full-duplex/half-duplex relaying with transmit power adaptation," *IEEE Trans. Wireless Commun.*, vol. 10, no. 9, pp. 3074–3085, Sep. 2011.

[27] I. Krikidis, H. A. Suraweera, S. Yang, and K. Berberidis, "Full-duplex relaying over block fading channel: A diversity perspective," *IEEE Trans. Wireless Commun.*, vol. 11, no. 12, pp. 4524–4535, Dec. 2012.

[28] H. Alves, D. B. da Costa, R. D. Souza, and M. Latva-aho, "On the performance of two-way half-duplex and one-way full-duplex relaying," in *Proc. IEEE 14th Workshop Signal Process. Adv. Wireless Commun. (SPAWC)*, 2013, pp. 56–60.

[29] H. Alves, D. B. da Costa, R. D. Souza, and M. Latva-aho, "Performance of block-Markov full duplex relaying with self interference in Nakagami-m fading," *IEEE Wireless Commun. Lett.*, vol. 2, no. 3, pp. 311–314, Jun. 2013.

[30] L. J. Rodriguez, N. H. Tran, and T. Le-Ngoc, "Performance of full-duplex AF relaying in the presence of residual self-interference," *IEEE J. Sel. Areas Commun.*, vol. 32, no. 9, pp. 1752–1764, Sep. 2014.

[31] S. Hong and G. Caire, "Virtual full-duplex relaying with half-duplex relays," *IEEE Trans. Inf. Theory*, vol. 61, no. 9, pp. 4700–4720, Sep. 2015.

[32] D. P. M. Osorio, E. E. B. Olivo, H. Alves, J. C. S. S. Filho, and M. Latva-aho, "Exploiting the direct link in full-duplex amplify-and-forward relaying networks," *IEEE Signal Process. Lett.*, vol. 22, no. 10, pp. 1766–1770, Oct. 2015.

[33] G. Liu, R. Yu, H. Ji, V. Leung, and X. Li, "In-band full-duplex relaying: A survey, research issues and challenges," *IEEE Commun. Surv. Tuts.*, vol. 17, no. 2, pp. 500–524, 2nd Quart. 2015.

[34] X. Cheng, B. Yu, X. Cheng, and L. Yang, "Two-way full-duplex amplify-and-forward relaying," in *Proc. IEEE Mil. Commun. Conf. (MILCOM)*, 2013, pp. 1–6.

[35] R. Vaze and R. W. Heath, "On the capacity and diversity-multiplexing tradeoff of the two-way relay channel," *IEEE Trans. Inf. Theory*, vol. 57, no. 7, pp. 4219–4234, Jul. 2011.

[36] D. Choi and J. Lee, "Outage probability of two-way full-duplex relaying with imperfect channel state information," *IEEE Commun. Lett.*, vol. 18, no. 6, pp. 933–936, Jun. 2014.

[37] H. Cui, M. Ma, L. Song, and B. Jiao, "Relay selection for two-way full duplex relay networks with amplify-and-forward protocol," *IEEE Trans. Wireless Commun.*, vol. 13, no. 7, pp. 3768–3777, Jul. 2014.

[38] Z. Cheng and N. Devroye, "The degrees of freedom of the K-pair-user full-duplex two-way interference channel with a MIMO relay," in *Proc. IEEE Int. Symp. Inf. Theory (ISIT)*, 2014, pp. 2714–2718.

[39] S. Tedik and G. K. Kurt, "Practical full duplex physical layer network coding," in *Proc. IEEE Veh. Technol. Conf. (VTC Spring)*, 2014, pp. 1–4.

[40] Z. Zhang, Z. Chen, M. Shen, and B. Xia, "On capacity of two-way massive MIMO full-duplex relay systems," in *Proc. IEEE Int. Conf. Commun. (ICC)*, 2015, pp. 4327–4332.

[41] H. Chen, G. Li, and J. Cai, "Spectral-energy efficiency tradeoff in full-duplex two-way relay networks," *IEEE Syst. J.*, pp. 1–10, 2015, doi: 10.1109/JSYST.2015.2464238.

Zhengquan Zhang received the M.Sc. degree in communication and information system from Southwest Jiaotong University, Chengdu, China, in 2008. He is currently pursuing the Ph.D degree at Southwest Jiaotong University. From July 2008 to December 2013, he was working with ZTE Corporation as a Communication Protocol Software Engineer. While working at ZTE, he participated in the development of 3G CDMA2000 1xEV-DO, and 4G LTE base station. He has submitted more than 20 patents. His research interests include co-operative communications, full-duplex radio, multiple access, radio resource management, and network architecture design.

Zheng Ma (M'07) received the B.Sc. and Ph.D degrees in communications and information system from Southwest Jiaotong University, in 2000 and 2006, respectively. He was a Visiting Scholar at the University of Leeds, Leeds, U.K., in 2003. In 2003 and 2005, he was a Visiting Scholar at Hong Kong University of Science and Technology, Hong Kong. From 2008 to 2009, he was a Visiting Research Fellow at the Department of Communication Systems, Lancaster University, Lancaster, U.K. He is currently a Professor with Southwest Jiaotong University, and serves as the Deputy Dean of the School of Information Science and Technology. He has authored more than 40 research papers in high quality journals and conferences. His research interests include information theory and coding, signal design and applications, FPGA/DSP Implementation, and professional mobile radio (PMR). He is currently the Editor for IEEE COMMUNICATIONS LETTERS. He is also the Vice Chairman of the Information Theory Chapter in the IEEE Chengdu section.

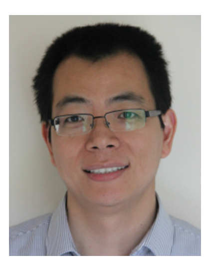

Zhiguo Ding (S'03–M'05–SM'15) received the B.Eng. degree in electrical engineering from Beijing University of Posts and Telecommunications, Beijing, China, in 2000, and the Ph.D degree in electrical engineering from Imperial College London, London, England, in 2005. From July 2005 to August 2014, he was working with Queen's University, Belfast, U.K., Imperial College, and Newcastle University, Newcastle upon Tyne, U.K. Since September 2014, he has been with Lancaster University, Lancaster, U.K., as a Chair Professor. From October 2012 to September 2016, he is also an Academic Visitor with Princeton University, Princeton, NJ, USA.

His research interests include 5G networks, game theory, co-operative and energy harvesting networks, and statistical signal processing. He is serving as an Editor for IEEE TRANSACTIONS ON COMMUNICATIONS, the IEEE TRANSACTIONS ON VEHICULAR TECHNOLOGY, the IEEE WIRELESS COMMUNICATION LETTERS, the IEEE COMMUNICATION LETTERS, and the *Journal of Wireless Communications and Mobile Computing*. He was the recipient of the Best Paper Award at the IET Communications Conference on Wireless, Mobile, and Computing, 2009, the IEEE Communication Letter Exemplary Reviewer 2012, and the EU Marie Curie Fellowship (2012–2014).

Ming Xiao (S'02–M'07–SM'12) received the Bachelor's and Master's degrees in engineering from the University of Electronic Science and Technology of China, Chengdu, China, in 1997 and 2002, respectively, and the Ph.D. degree from Chalmers University of Technology, Gothenburg, Sweden, in November 2007. From 1997 to 1999, he was a Network and Software Engineer with China Telecom. From 2000 to 2002, he also held a position in the Sichuan Communications administration. He has been with Department of Communication Theory, School of Electrical Engineering, Royal Institute of Technology, Stockholm, Sweden, since November 2007 where he is currently an Associate Professor of communications theory. He received the Hans Werthen Grant from the Royal Swedish Academy of Engineering Science (IVA) in March 2006, and Ericsson Research Funding from Ericsson in 2010. Since 2012, he has been an Associate Editor for the IEEE TRANSACTIONS ON COMMUNICATIONS, the IEEE COMMUNICATIONS LETTERS (Senior Editor since January 2015) and the IEEE WIRELESS COMMUNICATIONS LETTERS. He was the recipient of Best Paper Awards at the International Conference on Wireless Communications and Signal Processing in 2010 and the IEEE International Conference on Computer Communication Networks in 2011. He was also the recipient of the Chinese Government Award for Outstanding Self-Financed Students Studying Abroad in March 2007.

George K. Karagiannidis (M'96–SM'03–F'14) was born in Pithagorion, Samos Island, Greece. He received the University Diploma (5 years) and Ph.D. degree in electrical and computer engineering from the University of Patras, Patras, Greece, in 1987 and 1999, respectively. From 2000 to 2004, he was a Senior Researcher with the Institute for Space Applications and Remote Sensing, National Observatory of Athens, Greece. In June 2004, he joined the Faculty of Aristotle University of Thessaloniki, Thessaloniki, Greece, where he is currently a Professor with the Department of Electrical and Computer Engineering, and the Director of Digital Telecommunications Systems and Networks Laboratory. He is also an Honorary Professor with Southwest Jiaotong University, Chengdu, China.

His research interests include digital communications systems with emphasis on wireless communications, optical wireless communications, wireless power transfer and applications, molecular communications, communications and robotics and wireless security.

He is the author or coauthor of more than 400 technical papers published in scientific journals and presented at international conferences. He is also the author of the Greek edition of the book *Telecommunications Systems* and a coauthor of the book *Advanced Optical Wireless Communications Systems* (Cambridge, 2012). He has been selected as a 2015 Thomson Reuters Highly Cited Researcher.

Dr. Karagiannidis has been involved as a General Chair, a Technical Program Chair, and a Member of Technical Program Committees in several IEEE and non-IEEE conferences. In the past, he was an Editor of the IEEE TRANSACTIONS ON COMMUNICATIONS, a Senior Editor of the IEEE COMMUNICATIONS LETTERS, an Editor of the *EURASIP Journal of Wireless Communications & Networks* and several times a Guest Editor for the IEEE SELECTED AREAS IN COMMUNICATIONS. From 2012 to 2015, he was the Editor-in-Chief of the IEEE COMMUNICATIONS LETTERS.